Precipitation of Vacancies in Metals*

G. THOMAS AND J. WASHBURN
Department of Mineral Technology and Inorganic Materials Research Division, Lawrence Radiation Laboratory, University of California, Berkeley, California

1. INTRODUCTION

WITH the electron microscope one observes the structural changes resulting from an excess of point defects only *after* they have clustered, or collapsed into some kind of dislocation defect, e.g., loops, tetrahedra, and helices. Single vacancies have been detected by field ion microscopy (e.g., see Müller[1] and Brandon *et al.*[2]), but it seems improbable that single vacancies or very small groups can be resolved by electron microscopy. The smallest resolvable look is of the order of 50 Å diameter; smaller loops may appear as black dots or may even be invisible altogether since the strain fields on opposite sides of the loops tend to cancel each other. The presence of such strain fields renders defects visible in the electron microscope, provided certain geometrical conditions are satisfied. In terms of the diffraction contrast theory,[3,4] invisibility occurs when $\mathbf{g}\cdot\mathbf{R}$ is zero ($\mathbf{g}$ is the reciprocal lattice vector corresponding to the reflecting plane producing contrast, and $\mathbf{R}$ is the strain vector), i.e., when $\mathbf{R}$ lies in the reflecting plane (see Appendix B).

Whelan[5] has reviewed electron microscopy observations of clustered point defects up to 1961. Here we limit ourselves to clustered vacancies, considering the various factors involved in their precipitation, annihilation, and the manner in which vacancies induce hardening. An appendix is included as a practical guide towards analyzing dislocation loops formed from collapsed clustered point defects.

An excess of vacancies in a crystal may be produced as a result of quenching, irradiation, or plastic deformation. Quenching produces only vacancies, but the latter produce both vacancies and interstitials.

Since the concentration c of vacant atom sites in a crystal increases with increasing temperature by the relationship $c = A \exp(-E_f/kT)$, where A is an entropy factor ($\sim$1), E_f the formation energy of a vacancy ($\sim$1 eV), and k is Boltzmann's constant, very large vacancy concentrations may be produced by quenching materials rapidly ($>10^4$ deg sec^{-1}) from near the melting point. For Al with $E_f = 0.76$ eV,[6] the supersaturation is $\sim 10^9$ with $c \sim 10^{-4}$ just below the melting point. The supersaturation may be eliminated by diffusion of the vacancies to sinks (surfaces, dislocations) or by clustering and collapse into loops or other defects.[7–10] The energy of motion of the vacancy E_m is the energy barrier for an atom to jump into an adjacent vacant site. For example, taking E_m for Al = 0.54 eV [C. Panseri and T. Federighi, Phil. Mag. **3**, 1233 (1958), and W. De Sorbo and D. Turnbull, Acta Met. 7, 83 (1959)], vacancies will move at an appreciable rate at room temperature. In bcc metals, owing to the large values of E_f and small values of E_m, it has not been possible so far to quench bcc metals fast enough to observe defects.

A summary of the kinds of defects that have been observed by electron microscopy in quenched and aged metals is given in Table I (references 11–31).

2. FORMATION OF CLUSTERS

The growth of clusters during the early stages has been studied in copper, by x-ray small angle scattering (SAS), electrical resistivity (ER), and electron

* Review paper presented at the AIME Symposium on Point Defects, Dallas, Texas, February 1963.
[1] E. W. Müller, *Direct Observations of Imperfections in Crystals*, edited by Newkirk and Wernick (Interscience Publishers, Inc., New York, 1962), p. 77.
[2] D. G. Brandon, M. Wald, M. J. Southon, and B. Ralph, International Conference on Crystal Lattice Defects, Kyoto, Japan (1962). J. Phys. Soc. Japan (to be published).
[3] P. B. Hirsch, A. Howie, and M. J. Whelan, Phil. Trans. Roy. Soc. London **A252**, 499 (1960).
[4] A. Howie and M. J. Whelan, Proc. Roy. Soc. (London) **A263**, 217 (1961); Proc. Roy. Soc. (London) **A267**, 206 (1962).
[5] M. J. Whelan, *Electron Microscopy and Strength of Crystals*, edited by G. Thomas and J. Washburn (Interscience Publishers, Inc., New York, 1963), p. 3.
[6] F. J. Bradshaw and S. Pearson, Phil. Mag. **2**, 379, 570 (1957).
[7] A. H. Cottrell, Inst. Met. Rep Mon. Ser. No. 23, 1 (1958).
[8] F. Seitz and J. S. Koehler, *Solid State Physics*, (Academic Press Inc., New York, 1956), Vol. **2**, p. 305.
[9] P. Coulomb and J. Friedel, *Dislocations and Mechanical Properties of Crystals* (John Wiley & Sons, Inc., New York, 1957), p. 555.
[10] D. Kuhlmann-Wilsdorf, Phil. Mag. **3**, 125 (1958).

TABLE I. Summary of observations of quenching defects in metals and alloys.

Metal	Defect[a]	References
Al	P, F	11–13
Al-alloys	P, F, H, R	14–23
Ag	B, F, T	17, 18
Au	B, T	13, 24, 25
Ni	B, P (?)	26
Ni–Co	transition to tetrahedra P 60% Co	26
Cu	B, P, F, R, T	17, 18, 29, 30
Cu-alloys	B, R, P, F, (T?)	30, 31

[a] F Frank loop; P perfect loop; T tetrahedra; H helices; R rows of loops; B black spots (vacancy clusters ?)

microscopy (EM).[32,33] Chik *et al.*[32] suggest that divacancy migration is responsible for this clustering with a migration energy of $\lesssim$0.58 eV (Schule *et al.*[34]). Analyses of SAS measurements made in quenched Cu aged at, or slightly above, room temperature suggest that the clusters have spherical shapes[33] or perhaps are oblate ellipsoids.[32] Clusters are first detected by SAS after about 30 minutes aging at 25°C and reach a maximum size of ~30 Å (Fig. 25) after 2 hours. We have not resolved this stage of the clustering by EM. Cotterill[25] has suggested that the initial clusters in Au are also spherical, containing up to 400 vacancies.

The first observable defect in Cu after quench-aging is the so-called "black dot" effect of 50 Å diameter and larger (Fig. 1). More than one kind of black dot appears in copper and its alloys. Some of them may be due to contamination or surface effects produced during preparation of thin films. Black spots also form in the microscope due to bombardment by negative ions emitted from the cathode [D. W. Pashley and A. E. B. Presland, Phil. Mag. **6**, 1003 (1961)]. Seeger[32] has suggested that the smallest of these defects corresponds to the ellipsoid detected by SAS. Aging at 100°C produces clusters large enough to be resolved as dislocation loops. For the smallest loops that can be resolved it was not possible to decide whether they were of the Frank or the prismatic kind. This problem has been studied in aluminum by quenching single crystals of [111] orientation.[35] Figure 2 shows an example where, by contrast experiments, the loops all appear to be of the Frank kind.

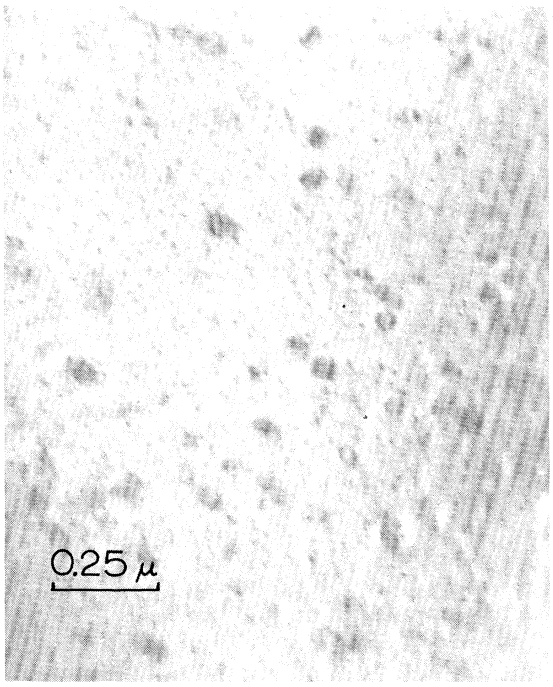

FIG. 1. Dislocation loops and "black dot" defect in O.F.H.C. copper quenched from 1000°C and aged 1 h at 100°C.

[11] P. B. Hirsch, J. Silcox, R. E. Smallman, and K. H. Westmacott, Phil. Mag. **3**, 897 (1958).
[12] D. Kuhlmann-Wilsdorf and H. G. F. Wilsdorf, J. Appl. Phys. **31**, 516 (1960).
[13] R. M. J. Cotterill and R. L. Segall, *Proceedings of the 5th International Congress on Electron Microscopy* (Academic Press Inc., New York, 1962), p. J-13.
[14] G. Thomas, Phil. Mag. **4**, 606, 1213 (1959).
[15] G. Thomas and M. J. Whelan, Phil. Mag. **4**, 511 (1959).
[16] K. H. Westmacott, D. Hull, R. S. Barnes, and R. E. Smallman, Phil. Mag. **4**, 1089 (1959).
[17] R. E. Smallman and K. H. Westmacott, J. Appl. Phys. **30**, 603 (1959).
[18] R. E. Smallman, K. H. Westmacott, and J. A. Coiley, J. Inst. Met. **88**, 127 (1959).
[19] R. B. Nicholson and J. Nutting, Acta Met. **9**, 332 (1961).
[20] G. L. Frank, D. L. Robinson, and G. Thomas, J. Appl. Phys. **32**, 1763 (1961).
[21] K. H. Westmacott, R. S. Barnes, D. Hull, and R. E. Smallman, Phil. Mag. **6**, 929 (1962).
[22] J. D. Embury, C. M. Sargent, and R. B. Nicholson, Acta Met. **10**, 1118 (1962).
[23] A. Eikum and G. Thomas, International Conference on Crystal Lattice Defects, Kyoto, Japan (1962). J. Phys. Soc. Japan (to be published).
[24] J. Silcox and P. B. Hirsch, Phil. Mag. **4**, 72 (1959).
[25] R. M. J. Cotterill, Phil. Mag. **6**, 1351 (1961).
[26] S. Mader, A. Seeger, and E. Simsch, Z. Metallk. **52**, 785, (1961).
[27] D. Kuhlmann-Wilsdorf, R. Maddin, and H. Kimura, Z. Metallk. **49**, 584 (1958).
[28] P. B. Hirsch and J. Silcox, *Growth and Perfection of Crystals* (John Wiley & Sons, Inc., New York, 1958), p. 262.
[29] R. M. J. Cotterill, Ph.D. thesis, Cambridge University, 1962.
[30] A. Eikum and G. Thomas, J. Appl. Phys. (in press).
[31] W. Bell and G. Thomas (to be published).
[32] K. Chik, A. Seeger, and M. Ruhle, *Proceedings of the 5th International Congress on Electron Microscopy* (Academic Press Inc., New York, 1962), p. J-11.
[33] J. Galligan and J. Washburn, UCRL Report No. 10606, Phil. Mag. (in press).
[34] W. Schüle, A. Seeger, F. Ramsteiner, D. Schumacher, and K. King, Z. Naturforsch. **16a**, 323 (1961).
[35] F. Vinçotte, J. Strudel, and J. Washburn (to be published).

Kuhlmann-Wilsdorf and Wilsdorf[12] suggest that the collapse, spherical → ellipsoid (void)→ loop, occurs initially due to elastic deformation of the material. Flattening of the ellipsoid occurs by surface diffusion of vacancies from the poles to the equator, and a loop forms when the void is flattened to 2 or 3 planes thick. This idea was used to explain their observations that loops in Al were often formed in groups which contained a high fraction of parallel loops.

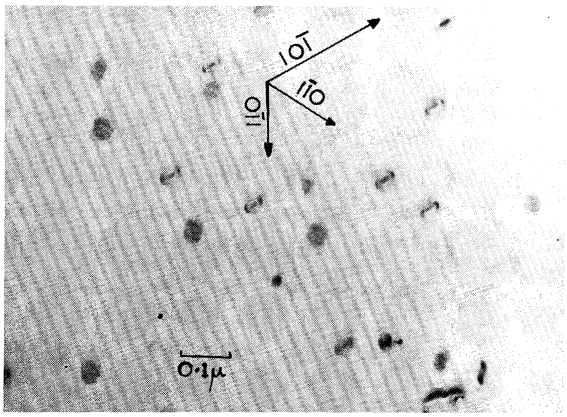

FIG. 2. [111] Al single crystal quenched from 600°C. Operating reflection $0\bar{1}1$. Notice that no loops are visible on (111) and ($\bar{1}11$) indicating that the loops are all of the stacking fault type with $a/3$ ⟨111⟩ Burgers vectors.

There is, therefore, good evidence that after quenching, single or divacancies cluster into equiaxed defects which subsequently collapse into loops. (See Sec. 6.)

3. NUCLEATING CONDITIONS

As shown in Table I, there have been numerous observations of quenching defects since the first published results of Hirsch *et al.* on Al.[11] The results of these observations may be summarized as follows:

(1) The distribution of loops is not always uniform.

(2) Small amounts of impurities or deliberate alloying additions inhibit formation of loops in varying degrees; often helices are the main defects in saturated (or nearly so) solid solutions.

(3) The dislocation loop densities in Cu, Ag, Ni, and alloys are often less than expected; in these cases loops are usually found near dislocation tangles.

(4) More than one kind of defect may be present in the same specimen.

(5) Plastic deformation *during quenching* may or may not favor loop nucleation. Associated with this is a specimen size factor.

(6) If quenching is followed immediately by low temperature deformation, loops are not observed in pure metals but are present in alloys, usually as columns. This suggests that loop nucleation is more difficult in alloys.

(7) A critical quenching temperature has been observed in Au and Al which is a function of impurity content.[13] Different kinds of defects are formed when material is quenched from above and below this temperature.

(8) As in all precipitation phenomena, homogeneous nucleation of defects is favored by high vacancy supersaturations (e.g., in displacement spikes formed by irradiation).

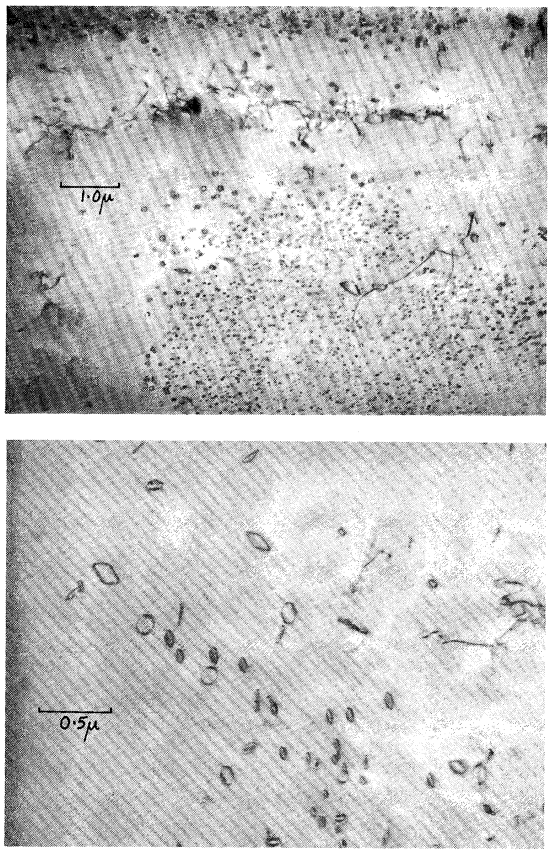

FIG. 3. (a) Showing colonies of loops in Al quenched from 600°C to −20°C, aged 5 sec 100°C (purity 99.999%). Notice larger loops at periphery of the colonies. (b) Enlarged view of edge of colony showing Frank loops as well as perfect diamond shaped loops.

The observations strongly suggest that the nucleation process is the most important factor in deciding the number, kind, and distribution of defects. Defects may form by homogeneous and heterogeneous precipitation. We now consider some of the factors listed above.

(a) Effect of Deformation

The really critical deformation experiments have yet to be done in which the quench rate, specimen size, and deformation effect are investigated in single crystals. Quenching polycrystals with so-called zero deformation is not possible. One reason for this is due to the anisotropy of the coefficient of expansion at and near grain boundaries; differential stresses will be set up which could multiply dislocations. Furthermore, crystals are not dislocation-free prior to quenching. Figure 3 shows photographs of polycrystalline Al, in which colonies of densely populated loops are surrounded completely by loop-free regions. These free regions may correspond with the three dimensional cell arrangements of dislocations present prior to quenching.[35] This is borne out by the variation in size of loops, the smallest being at the center and largest ones at the fringes of the colonies [Fig. 3(b)] as expected if the precipitation was homogeneous in areas of varying vacancy concentration. Loop-free regions can also result from plastic deformation during quenching, or after quenching and aging [R. Vandervoort and J. Washburn, Phil. Mag. **5**, 24 (1960)]. This is consistent with the fact that loop-free areas sometimes correspond with the traces of slip planes. Destruction of loops by moving dislocations is shown in Fig. 4.

(b) Impurity Effects

The situation with regard to impure metals or alloys is further complicated because of the presence of solute atoms. Single vacancies and vacancy aggregates of all sizes may be associated with impurity atoms and impurity atom clusters. The binding energy between the solute atom and a vacancy, E_b, then becomes an important parameter.

The nucleation of defects and the resulting growth processes may obviously be modified as compared to the pure metal. It is in these cases that heterogeneous nucleation has been positively identified. Even the small amounts of impurities found in most so-called "pure" metals can have a pronounced effect both on the nucleation rate and mode of precipitation. Cotterill and Segall[13] suggest that the ratio c/n is an important factor, where c is the vacancy and n the impurity concentration. However, Federighi and Thomas[36] show that the c/n ratio should be important only if E_b is not too small. For sufficiently high ratios, or low values of E_b, homogeneous nucleation is still possible, but for high values of E_b only heterogeneous nucleation may be possible. For low c/n and high E_b the vacancies may be permanently trapped by the impurities. The solute atoms themselves may cluster as in many aluminum alloys.[37] Both vacancies and solute atoms may be at the defects. This leads to accelerated heterogeneous precipitation of a solid phase, as has been found in Al–Cu (θ')[38,39] and Al–Ag (γ') alloys.[19,20,40,41] The c/n ratio falls exponentially with decreasing quenching temperature (since only c changes). Besides having fewer total vacancies available for precipitation, those formed may all be trapped when the quenching temperature is lowered. Cotterill and Segall found that 99.98% pure Au quenched from 1000°C produced black spot defects whilst 99.999% pure Au formed fewer but larger tetrahedra under the same conditions. They also found that 99.995% pure Al formed prismatic loops but 99.999% pure Al formed Frank loops of larger diameter. The 99.995% pure Al was made to behave in the same way as 99.9999% pure Al by repeatedly heating and quenching the former. This latter effect was explained as a purification process occurring within about 0.01 cm of the specimen surfaces. These observations suggest that small amounts of impurity may provide sites for heterogeneous precipitation of vacancies. When E_b is high and c/n is large, solute atoms may increase the number of vacancy clusters that are formed. The effect of alloying on quenching

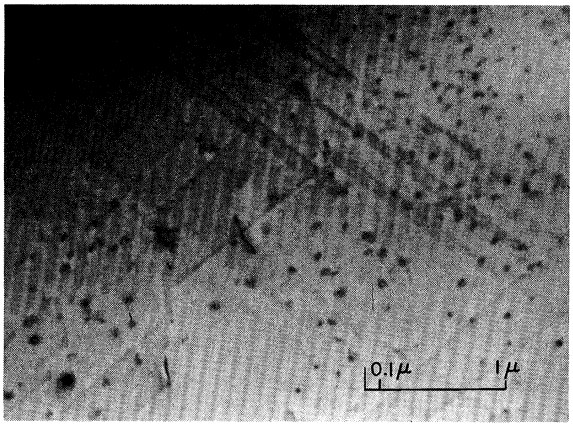

FIG. 4. Motion of dislocations with large jogs acquired by annihilation of loops (Courtesy ASM "Strengthening Mechanisms in Solids" 1962, p. 64).

[36] T. Federighi and G. Thomas, Phil. Mag. **7**, 127 (1962).

[37] R. B. Nicholson, G. Thomas, and J. Nutting, J. Inst. Metals **87**, 429 (1959).

[38] G. Thomas and M. J. Whelan, Phil. Mag. **6**, 1103 (1961).

[39] G. Thomas and J. Nutting, Acta Met. **7**, 315 (1959).

[40] R. B. Nicholson, *Electron Microscopy and Strength of Crystals* (Interscience Publishers, Inc., New York, 1962), p. 861.

[41] J. A. Hren and G. Thomas, Trans AIME, **227**, 308 (1963).

defects has been investigated for a number of Al alloys by Thomas.[14] In Al–Zn alloys where $E_b \sim 0.06$ eV (see Table II) there is practically no effect of zinc additions even up to 30% (e.g., compare Fig. 5 with Figs. 2 and 3). In Al–Mg, however, with $E_b \sim 0.1$–0.4 eV, vacancy precipitation may be suppressed altogether in the Al–7% Mg alloy. In Al–Cu ($E_b \simeq 0.2$ eV) and Al–Ag ($E_b \simeq 0.2$ eV) similar effects occur. Westmacott *et al.*[21] also concluded that vacancy trapping occurs in Al alloys.

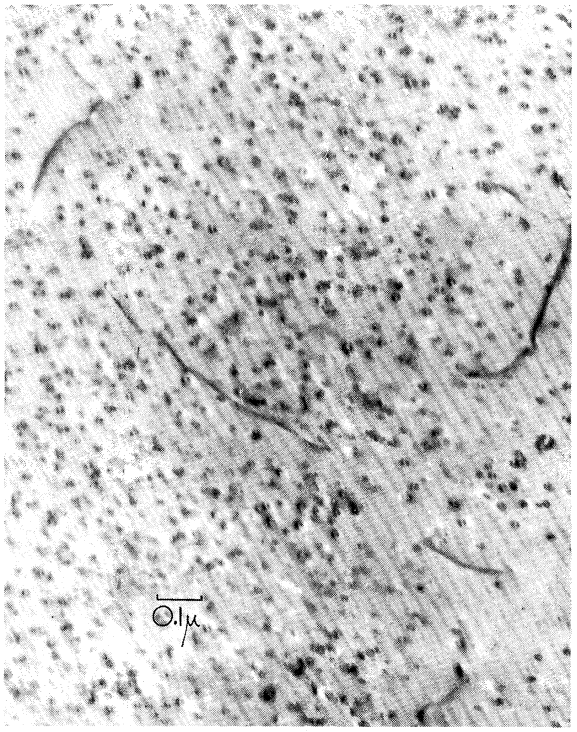

FIG. 5. Al–10% Zn alloy quenched from 580°C[14] (courtesy Phil. Mag).

Embury *et al.*[22] and Eikum and Thomas[23,30] showed that in alloys where there is strong vacancy trapping (i.e., when homogeneous precipitation is difficult) plastic deformation during or immediately after quenching facilitates precipitation of vacancies into loops, many of which are aligned in columns [Fig. 6(a)]. Dislocations introduced by the plastic deformation are, therefore, effective in causing heterogeneous precipitation. The precipitated vacancy concentration (estimated from the density and size of loops) is larger by an order of magnitude in quenched-deformed Al–5% Mg alloy than in an *as*-quenched specimen[23] [Fig. 6(b)].

The effects of O_2 are very strong in silver and probably in copper and the noble metals. N_2 and H_2

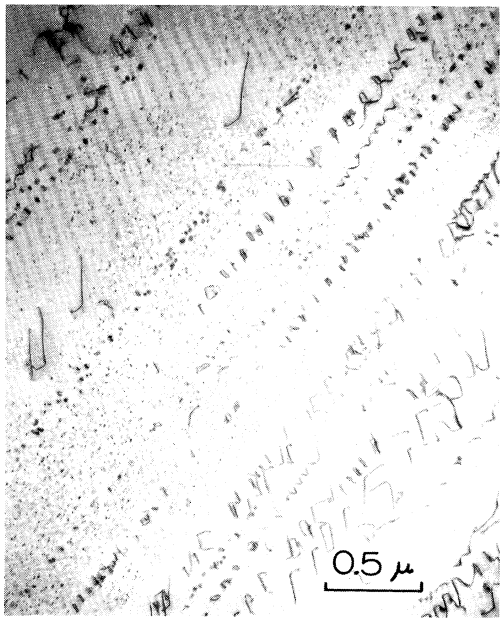

(a)

may also be important, and there is evidence that He, Ne, and other gases can permeate through copper. It is known that hydrogen is soluble in liquid Al, so it may be that gaseous atoms are important impurities in the "pure" metals. Discrepancies in the

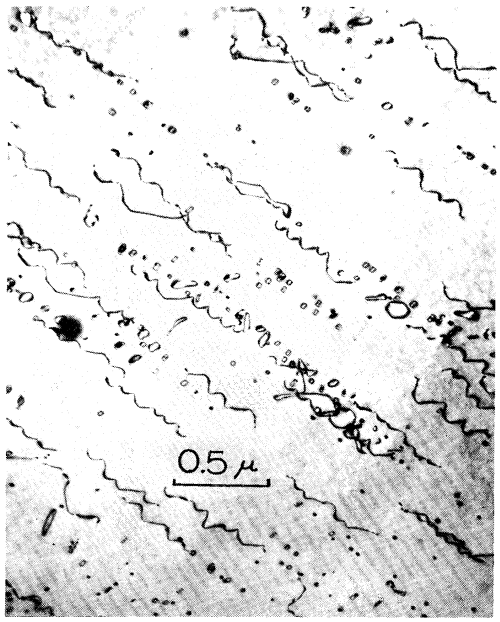

(b)

FIG. 6. (a) Al–5% Mg alloy quenched from 550°C deformed 3% aged 11 min at 20°C and further deformed 11%. Notice columns of large loops aligned along ⟨110⟩. (b) Al–5% Mg alloy quenched from 550°C. Comparison with Fig. 6(a) shows that the helices present here break down into loops as a result of deformation.

various experimental results may thus be attributed mainly to these impurities.

Table II shows some values of the binding energies determined by quenching experiments.

A critical factor influencing nucleation is, therefore, the fraction of vacancies trapped by solute atoms. This is represented in Fig. 7. Impurities or solute atoms are effective in *decreasing* the supersaturation of vacancies leading eventually to no precipitation. The phenomena can be understood in terms of the phase equilibria between vacancies, solute atoms, and solvent atoms.

The association of solute atoms with vacancy clusters may also determine what kind of defect is formed, i.e., a Frank or prismatic loop. Thus, in Al–Ag alloys[19,20,40] Frank loops and dissociated helices are stabilized because of the segregation of silver atoms.

TABLE II. Binding energies between vacancies and solute atoms.

System	Exp. Method	E_b (eV)	Reference
Al–Sn	ER	0.4[a]	42
Al–Mg	ER, EM	0.1–0.4[a]	23, 43, 44
Al–Cu	ER	0.2	45
Al–Zn	ER, EM	0.06	14, 74
Al–Ag	SAS	0.4[a]	46
Ag–O	ER	0.4	47
Fe–C	IF	not det.	48
Cu–O	EM	not det.[b]	30
Cu–Ag	EM	not det.[b]	31
Cu–Al	EM	not det.[b]	31
Cu–Au	EM	not det.[b]	31
Cu–Zn	EM	not det.[b]	31

[a] Maximum value.
[b] Expected to be large because very few defects are observed.

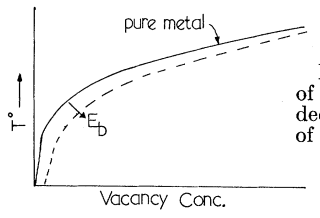

FIG. 7. Schematic illustration of the effect of impurity atoms in decreasing the supersaturation of vacancies when $E_b \neq 0$.

4. HELICAL DISLOCATIONS

In the presence of a nonequilibrium concentration of vacancies, dislocations, particularly those near screw orientation, tend to climb into a helical shape.[49] The number of vacancies that must be absorbed to produce one turn of a helix is the same as that to form one prismatic loop of the same diameter. Therefore, to form a helix of many turns having a diameter large enough to be easily recognized by transmission electron microscopy, a large number of vacancies must be absorbed (Figs. 8, 9). This is most likely to occur when other sinks for excess vacancies are not nucleated (e.g., in alloys having an appreciable binding energy between vacancies and solute atoms, or on quenching from a temperature too low to achieve the critical supersaturation for nucleation of vacancy clusters).[14,15] We have observed helical dislocations in pure aluminum but they are unstable under observation in thin foils. X-ray diffraction topographs reveal large scale helices in annealed pure aluminum.[50] Long, perfect helices are particularly stable when E_b is large.[14] Solute elements associated with the dislocation line help to prevent glide of segments of the dislocation line, which can lead to degeneration of the helix. A helix is converted into a row of prismatic loops when a screw dislocation of opposite Burgers vector combines with it [Fig. 6(a)]. This can be caused by stress-induced bowing of a

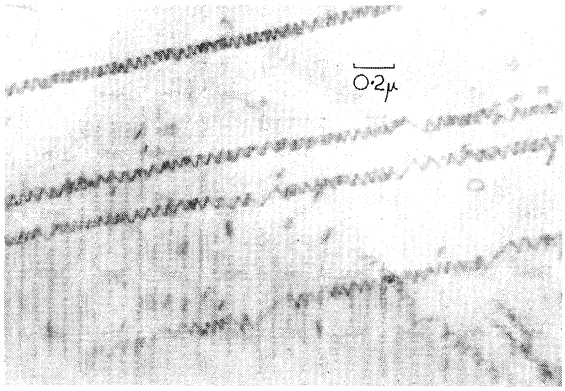

FIG. 8. Long regular helices in Al–4% Cu after quenching from 540°C[15] (courtesy Phil. Mag.).

[42] H. Kimura and R. R. Hasiguti, International Conference on Crystal Lattice Defects, Kyoto, Japan (1962). J. Phys. Soc. Japan **18**, Suppl. 111, 73 (1963).
[43] J. Takamura, K. Okazaki, and I. G. Greenfield, International Conference on Crystal Lattice Defects, Kyoto, Japan (1962). J. Phys. Soc. Japan **18**, Suppl. 111, 78 (1963).
[44] J. D. Embury and R. B. Nicholson, Acta Met. **11**, 347 (1963).
[45] H. Kimura, A. Kimura, and R. R. Hasiguti, Acta Met. **10**, 607 (1962).
[46] R. Bauer and V. Gerold, Z. Metallk. **52**, 671 (1961).
[47] Y. Quere, International Conference on Crystal Lattice Defects, Kyoto, Japan (1962). J. Phys. Soc. Japan **18**, Suppl. 111, 91 (1963).
[48] F. E. Fujita and A. C. Damask, International Conference on Crystal Lattice Defects, Kyoto, Japan (1962). J. Phys. Soc. Japan **18**, Suppl. 111, 105 (1963).
[49] S. Amelinckx, W. Bontinck, W. Dekeyser, and F. Seitz, Phil. Mag. **2**, 355 (1957).
[50] A. R. Lang and G. Meyrich, Phil. Mag. **4**, 878 (1959).

particularly large turn of the helix itself, the gliding segment folding back on the other turns of the helix. In this way, one or any number of turns of a helix can be converted into loops. Loops can also result from growing together of two adjacent helices of opposite sign. In the latter case, very irregular loops and loops of twice the original helix cross section can be produced as has been observed in Al–Cu.[15]

Columns of loops may also be produced by a completely different mechanism than described above, viz., by prismatic punching, as was shown originally by the experiments of Jones and Mitchell.[51] If a material contains a second phase (e.g., inclusions or precipitates) the differential thermal contraction

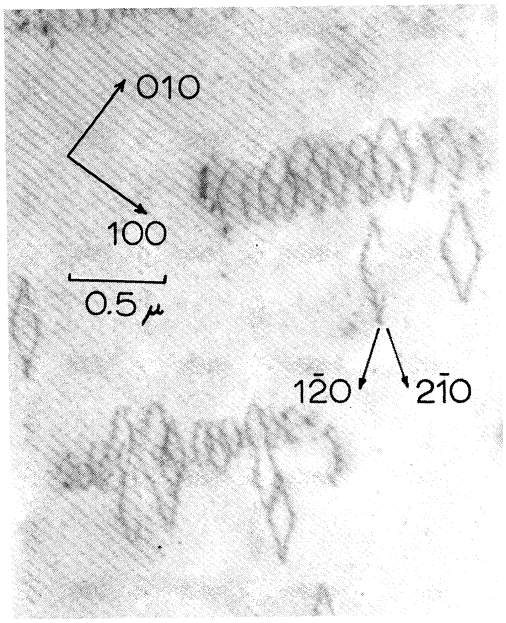

FIG. 9. Diamond-shaped loops and helices in Al–5% Mg quenched from 520°C and aged 94 h at 100°C. The most probable plane of the loops is (111) or ($\bar{1}\bar{1}$1).

arising during quenching sets up stresses at the particle–matrix interface, which can be relieved by punching out loops. Since the coefficients of thermal expansion of intermetallic compounds are generally smaller than those of metals, loops would be expected to be of the interstitial kind. If these are formed, their size would decrease with distance from the source due to annihilation by combination with vacancies. This effect is illustrated for a Cu–$\frac{1}{2}$% Ag alloy in Fig. 10 and for grain boundary precipitates of Mg_3Al_2 in Al–5% Mg alloy in Fig. 11. Similar

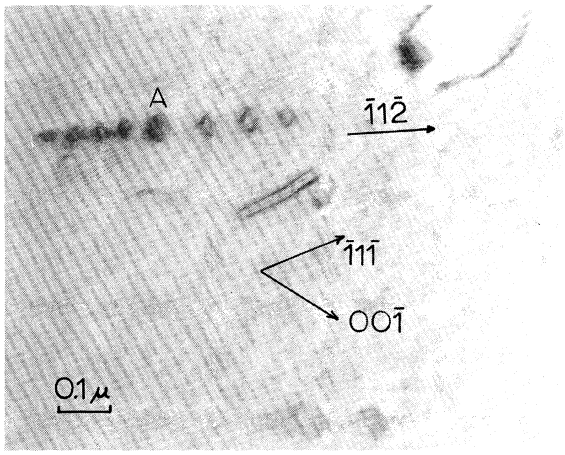

FIG. 10. Cu–0.5 at. % Ag quenched from 1065°C and aged 1 h at 100°C, showing a row of loops punched from the region A. The loops diminish in size with distance from the origin indicating that they are of the interstitial type.

results have been obtained by Partridge and Lally[52] for quenched Mg, and in quenched copper by Barnes and Mazey[53] who further showed that the spacing between loops in the columns was consistent with the theory of Bullough and Newman.[54]

Precipitates also give rise to loops which are not

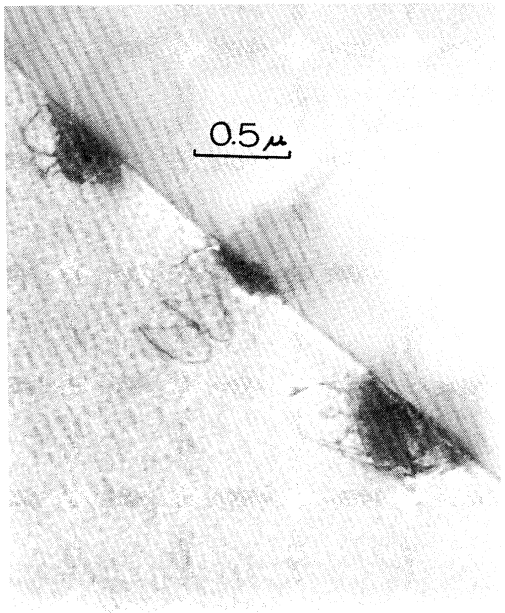

FIG. 11. Al–5 wt. % Mg quenched from 520°C and aged 70 h at 100°C, showing dislocation sources and punched loops originating from precipitates in the grain boundary.

[51] D. A. Jones and J. W. Mitchell, Phil. Mag. **3**, 1 (1958).

[52] J. S. Lally and P. G. Partridge, *Proceedings of the 5th International Congress on Electron Microscopy* (Academic Press Inc., New York, 1962), p. J-12.

[53] R. S. Barnes and D. J. Mazey, U.K. AERE Report No. R4126, 1962. Acta Met. **11**, 281 (1963).

[54] R. Bullough and R. C. Newman, Phil. Mag. **5**, 921 (1960).

formed by prismatic punching. These have been described as climb sources and are discussed in Appendix A.

5. CLUSTERED VACANCIES PRODUCED BY IRRADIATION

If a metal is bombarded with material particles of sufficient momentum, many atoms can be ejected from their lattice points leaving clustered vacancies in this region (Brinkman displacement spike[55]). Thus, heavy particles, such as neutrons or α particles, produce vacancy clusters at a primary collision, whereas light particles (e.g., electrons) produce clusters only if the temperature is high enough for vacancy diffusion to occur. If a displacement spike is produced without subsequent diffusion, there will be no denudation of clusters near sinks. Figure 12 is an example of displacement spikes in high purity Nb irradiated at liquid nitrogen with 3-keV Cs ions (total dose 2×10^{17}). The largest loops have diameters $\sim$150 Å. Associated with low angle boundaries, helices and rows of loops are observed. The appearance of double helices suggests that punching from the boundary may have occurred. An example is shown in Fig. 13.

On the other hand, 38-MeV α-particle bombardment of copper at 200°C produces irregular loops of $\sim$400-Å diameter with denudation near grain boundaries, indicating that point defect diffusion has occurred during irradiation.[56] Experiments with He gas injection, which results in precipitation of gas bubbles by attracting vacancies from sources such as loops, showed that loops expand during this process; hence, loops must be of the interstitial kind.

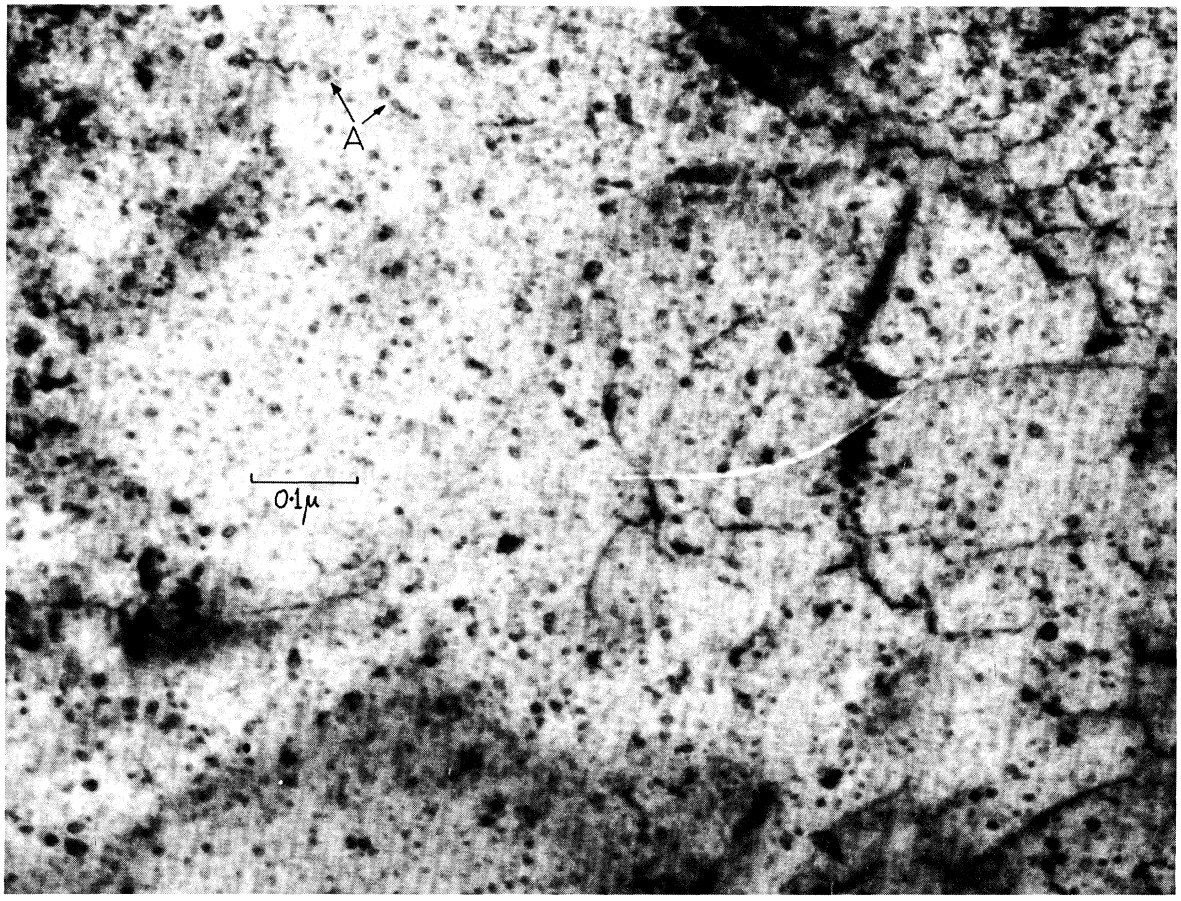

FIG. 12. High purity Nb annealed 1780°F and bombardment with 2×10^{17} Cs ions cm^{-2} (3.0 keV) at liquid nitrogen. Loops can be resolved at A (courtesy L. E. Thomas, Rocketdyne).

[55] J. S. Brinkman, Am. J. Phys. **24**, 246 (1956).

[56] R. S. Barnes, Discussions Faraday Soc. **31**, 38 (1961).

Similar effects have been observed in Fe and Ag. α-particle damage to Al also produces mainly interstitial loops.[57]

Castaing and Jouffrey[58] have investigated argon ion bombardment in thin evaporated gold films and observed vacancy loops which could be eliminated by annealing, either during or subsequent to bombardment.

In neutron damage, both vacancy clusters ("black dots") and precipitated disks of interstitial atoms (loops) have been recognized in copper.[56,59] The clusters correspond to displacement spikes but the interstitial loops result from diffusion. Barnes concludes that little recombination of vacancies and interstitials occurs until very high neutron doses are reached.[56] Annealing experiments show that the black dots are extremely stable configurations. While they consist of vacancies and should disappear at 350°C, they persist even above 500°C. During aging, growth occurs, enabling the "spots" to be resolved as tetrahedral defects. Such tetrahedra are very stable (e.g., in Au), thus explaining their persistence. Furthermore this also explains the nonexchange vacancy $\leftrightarrow$ interstitial upon annealing.

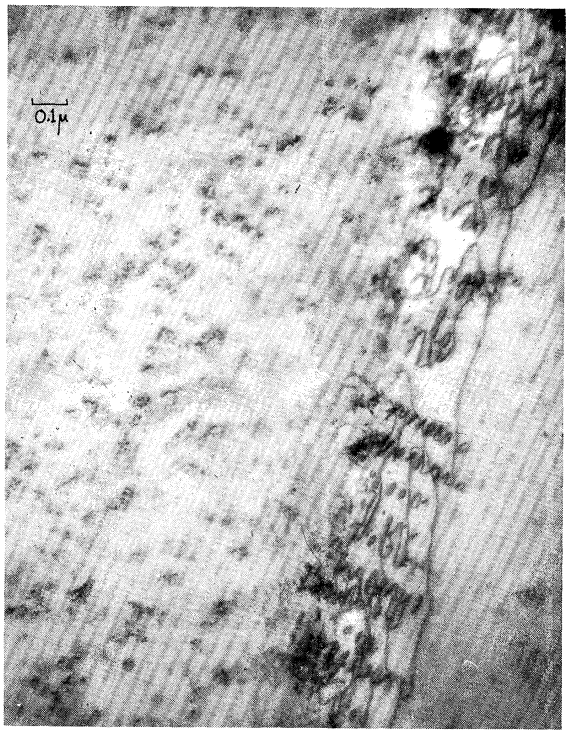

FIG. 13. As Fig. 12, showing helices and rows of loops emitted from a boundary. Notice clusters of black spot defects (courtesy L. E. Thomas, Rocketdyne).

Westmacott *et al.*[60] recently examined thin films of zone-refined Al after bombardment at 80°C with a flux of 1.6×10^{10} fission fragments cm^{-2} sec^{-1}. Defects were first observed after 30 sec dose and these grew with time into loops on {110} with ⟨110⟩ Burgers vectors. It appears that both vacancy and interstitial clusters form during the bombardment. Initially, each type of defect attracts its own kind and repels the other. Growth occurs independently by climb and slip. Loops of opposite kind were also observed to slip together and cancel. This work shows that growth of loops can occur in part by loop migration through slip and, perhaps, conservative climb, and does not (in this case) take place entirely by random migration of single defects. The gliding together of small perfect loops has also been observed in Au,[61] Pt,[62,63] and U.[64] In cases where the loops are imperfect (Frank kind) slip cannot occur so that loops will not come together unless the temperature is high enough to allow conservative climb to take place.

Recent information regarding the nature of interstitial defects produced by irradiation in various materials can be found in reference 65.

6. NUCLEATION AND GROWTH MECHANISMS

The relative energies of the three types of defect (stacking fault tetrahedron, stacking fault loop, and perfect loop) that could be formed from a given number of vacancies can be estimated if the stacking fault energy for the crystal is known. They are given approximately by:

$$E_L = \frac{Ga^2 l}{4\pi(1-\nu)} \ln\left(\frac{l}{r_0}\right) + \frac{\sqrt{3}}{4} l^2 \gamma ,$$

$$E_T = \frac{Ga^2 l}{12\pi(1-\nu)} \ln\left(\frac{l}{r_0}\right) + \sqrt{3}\, l^2 \gamma ,$$

$$E_P = \frac{Ga^2 l}{2.4(1-\nu)} \ln\left(\frac{2l\sqrt{2}}{a}\right) ,$$

where E_L, E_T, and E_P are the energies of a triangular

[57] D. J. Mazey, R. S. Barnes, and A. Howie, Phil. Mag. **7**, 1861 (1962).
[58] R. Castaing and B. Jouffrey, J. de Mic. **1**, 201 (1962).
[59] D. J. Makin, A. D. Chapman, and F. J. Minter, Phil. Mag. **6**, 465 (1961).
[60] K. H. Westmacott, A. C. Roberts, and R. S. Barnes, Phil. Mag. **7**, 2035 (1962).
[61] D. G. Brandon and P. Bowden, Phil. Mag. **6**, 707 (1961).
[62] A. J. Baker, Discussions Faraday Soc. **31**, 72 (1961).
[63] E. Ruedle, P. Delavignette, and S. Amelinckx, *Proceedings of the 5th International Congress on Electron Microscopy* (Academic Press Inc., New York, 1962), p. F-2.
[64] B. Hudson, K. H. Westmacott, and M. J. Makin, Phil. Mag. **7**, 377 (1962).
[65] *Proceedings of the 5th International Congress on Electron Microscopy* (Academic Press Inc., New York, 1962), pp. F-1 to G-14.

stacking fault loop, a tetrahedron, and a triangular perfect loop respectively, each having side l. G is the shear modulus, a the unit cell dimension, r_0 the dislocation core radius, ν is Poisson's ratio, and γ is the stacking fault energy.

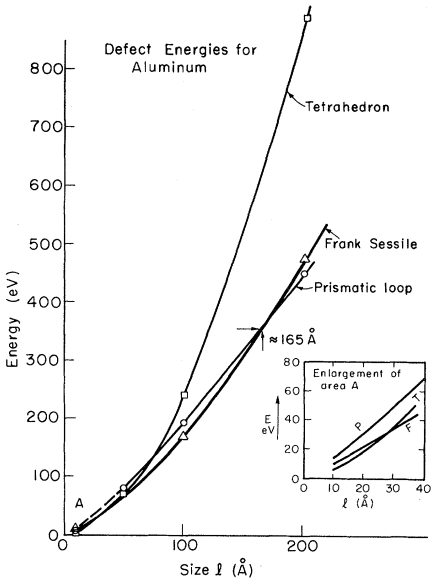

FIG. 14. Al: Energy of defects as a function of size.

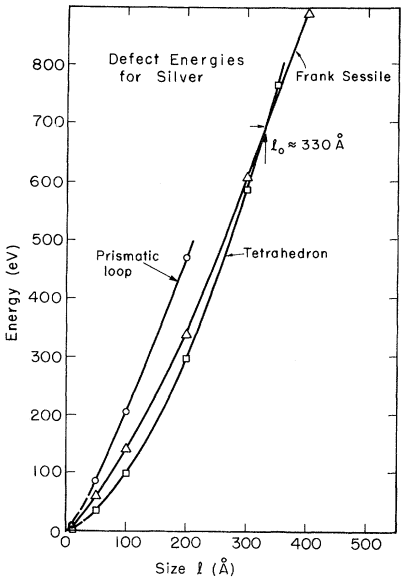

FIG. 15. Ag: Energy of defects as a function of size.

These relative energies are shown as a function of l in Figs. 14 and 15 for aluminum and silver, respectively.[30] The perfect loop always has lowest energy above an upper critical size, and the tetrahedron is always favored below a lower critical size. Between these two values of l the Frank loop is stable. Table III lists the lower critical value $l = l_0$ for a number of metals along with the stacking fault energies chosen in making the calculation. The results obtained are sensitive to the chosen value for γ, and there is still doubt concerning the accuracy of the values given in the Table.

It is obvious from the experimental observations that these simple energy comparisons do not always determine the type of defect that is present. For example, copper and aluminum may both show Frank loops (Fig. 16) even though γ for Al is thought to be four or five times larger than that of Cu. As shown in Table I, more than one type of defect is often found in the same metal and the dimensions of the defects are frequently outside the predicted range of stability. However, the observations do follow the predictions in a general way. Tetrahedra are observed (Fig. 17) when the stacking fault energy is low and perfect loops are found more frequently in aluminum than in any other metal.

TABLE III. Calculated values of the maximum size of tetrahedra below which this is the most stable defect.

	G dyn/cm^2	γ ergs/cm^2	a Å	l_0 Å
Au	2.7×10^{11}	33	4.0787	430
Ni	7.8×10^{11}	95	3.5234	330
Ag	2.6×10^{11}	40	4.08	330
Cu	4.5×10^{11}	40	3.6147	515
Pb	0.75×10^{11}	50	4.9502	83
Cu–Zn	4.5×10^{11}	20	4.0450	1.6×10^4
Ag–Al	2.4×10^{11}	1	4.0643	2×10^5
Al	2.5×10^{11}	180	4.05	28

To understand the occurrence of defects having dimensions outside the predicted range of stability it is necessary to assume either that the value of stacking fault energy chosen is incorrect or that there is a large enough activation energy in the process of conversion of one type of defect to another to make the frequency of conversion negligible. In most cases, the latter explanation appears to be the most reasonable. Saada[66] has considered the transformation of stacking fault loops to perfect loops by nucleation of a loop of Shockley partial in the stacking fault. He finds that even in aluminum large stacking fault loops may not transform. A stress aids the nucleation of a Shockley partial. Although the formation of perfect loops in aluminum may be due to stresses, there is some doubt as to how many of the small loops observed in Al are really perfect

[66] G. Saada, Acta Met. **10**, 551, 985 (1962).

(e.g., see Fig. 2). Stress aided transformation to perfect loops has been observed in the electron microscope (Yoshida, private communication). The stress in this case is caused by local heating of the specimen by the electron beam.

Small angle scattering experiments on copper[33] indicate that there is a continuous increase in the size of defects within the range of 10 to 30 Å. The measurements also indicate that the defects are approximately equiaxed rather than plate-shaped or rod-shaped. From about 30 to 100 Å the defects are visible in thin foils as "black spots." When these black spots grow to a size that can just be resolved, they are found to have a tetrahedral shape in copper.[56] These observations, along with the energy considerations given above, suggest that many vacancy clusters grow initially as tetrahedra. We propose that, in the case of aluminum, these transform to stacking fault loops by nucleation of a Shockley partial at one of the corners before they reach a size that is visible by transmission electron microscopy and that during further growth the shape changes from triangular to hexagonal. For gold the activation energy for the transformation, tetrahedron → Frank loop, must be large enough to prevent the transformation, even for tetrahedra well above the critical size.[25]

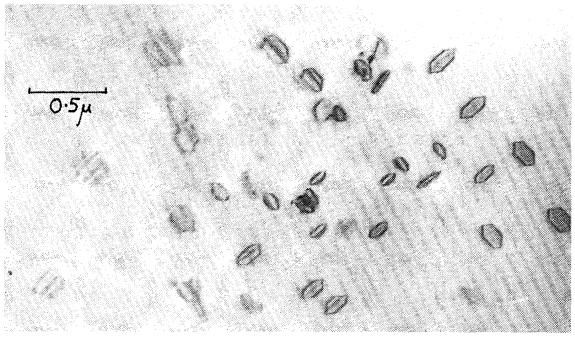

(a)

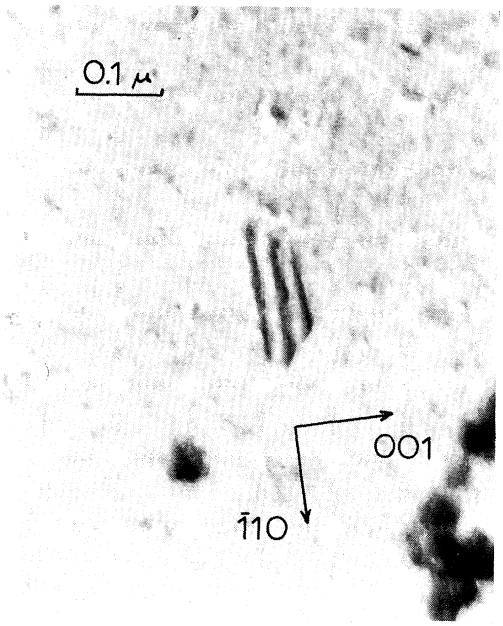

(b)

FIG. 16. (a) Frank loops in Al purity 99.999% quenched from 600°C to −20°C aged 5 sec 100°C. (b) A large truncated hexagonal Frank loop in Cu–2 at. % Ag quenched from 1000°C and aged 1 h at 100°C.

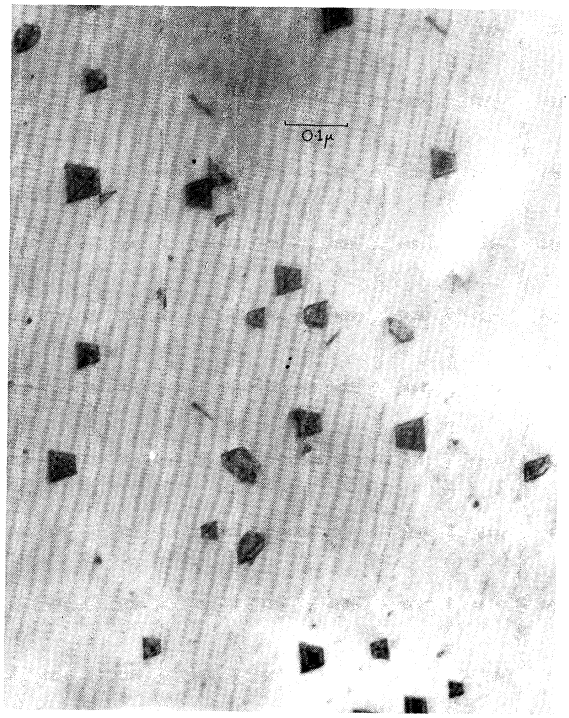

FIG. 17. Tetrahedra in quenched gold; after Silcox and Hirsch[24] (courtesy Phil. Mag.).

Continuous growth of tetrahedral defects has also been suggested recently by Czjzek *et al.*[67] and de Jong and Koehler.[68] The latter authors suggest that a cluster of six vacancies can collapse directly to form a stacking fault tetrahedron and that single vacancies can be absorbed at its edges producing steps in the stacking fault faces. They suggest that the nucleation of tetrahedra in gold probably takes place by the addition of a divacancy to a quadravacancy or a single vacancy to a pentavacancy. The

[67] C. Czjzek, A. Seeger, and S. Mader, Max-Planck (Stuttgart) Report 1962.
[68] M. de Jong and J. S. Koehler, Phys. Rev. **129**, 49 (1963).

quadravacancy was considered to be the smallest cluster that would not be in equilibrium with single and divacancies.

The effect of solute elements may be to decrease the stability of one of the links in the chain such as the quadravacancy or pentavacancy and, therefore, make nucleation more difficult. Alternatively, they may inhibit the addition of single vacancies to the edges of a tetrahedron and thereby prevent their rapid growth. The occurrence of perfect loops in copper may, therefore, be due to impurity atoms

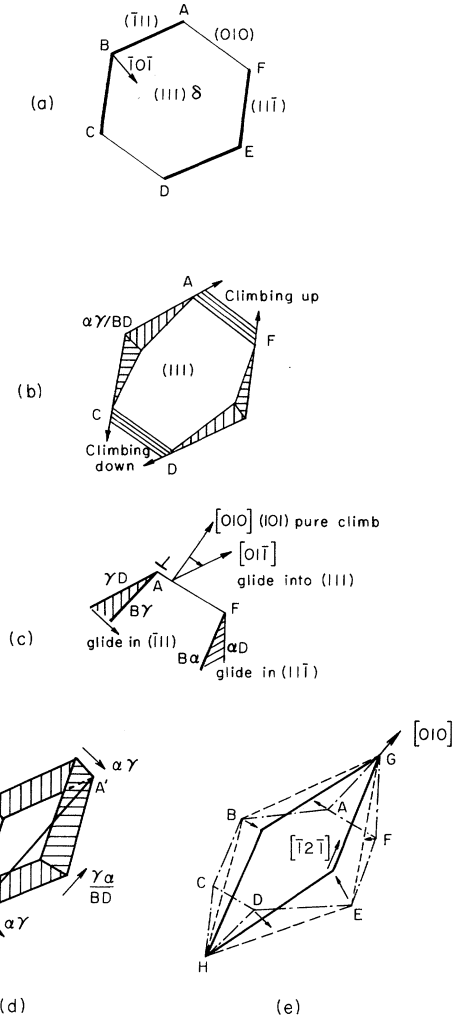

FIG. 18. Schematic representation of formation of diamond shaped loops from hexagonal loops [e.g., see Figs. 3(b), 9].

which influence the manner in which vacancies cluster as well as affecting the vacancy supersaturation. Alternatively perfect loops may be formed by a different mechanism (e.g., by degeneration of helical dislocations or by collapse of voids).

In Al (and some Al alloys) large perfect diamond-shaped loops are often found in regions where the vacancy supersaturation was small, e.g., near sinks [Fig. 3(b)]. Associated with these loops, large Frank loops are also observed. The sequence of vacancy

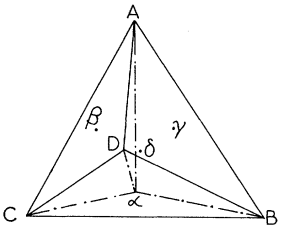

FIG. 19. Tetrahedron of {111} planes in the fcc lattice; the Burgers vectors of dislocations AB, BC, CD, DA are $a/2$ ⟨110⟩; Aγ, Bγ etc. $a/6$ ⟨211⟩; $\gamma\beta$,$\alpha\gamma$ etc. $a/6$ ⟨110⟩; and Aα, Cγ etc. $a/3$ ⟨111⟩.

clustering, collapse, and growth of defects to form these diamond-shaped loops might be as follows:

> tetrahedron → triangular Frank loop → growth to hexagonal Frank loop → hexagonal perfect loop → growth into perfect diamond loop.

When the tetrahedron reaches a critical size, nucleation of a Shockley loop at one of the corners sweeps away three of the stacking faults and three of the stair-rod dislocations. This process may be aided by the steps which must be present in the stacking faults during its growth. These additional stair-rod dislocations decrease the stability of the tetrahedron. Degeneration of a tetrahedron results in a triangular Frank loop. As these loops continue to grow by absorption of additional vacancies, the shape would be expected to change from triangular to hexagonal. As the three sides of the triangle climb outward, new straight segments will be formed at the corners eliminating the acute angles so as to require a minimum increase in length of the dislocation. Some of the large Frank loops are then transformed to perfect hexagonal loops by nucleation of a Shockley partial. Since diamond-shaped perfect loops most often appear near dislocation tangles, the stress fields of nearby dislocations may aid the transformation. If growth continues after the hexagonal loop becomes perfect, climb of the six sides will no longer be symmetrical.

Consider a perfect loop, ABCDEF, as shown in Fig. 18(a) with Burgers vector $\frac{1}{2}a[\bar{1}0\bar{1}]$.[30] The relationship between the {111} planes and all possible Burgers vectors is shown in Fig. 19. The segments AF and CD of Fig. 18 lie in (010) and are pure edge but cannot glide. These can, however, climb and the corners A and F act as nodal points. It is possible for the segments along FE, ED, CB, and BA to dissociate as follows [Fig. 18(b)]:

segment FE $\quad BD \rightarrow B\gamma + \gamma D$ on $(11\bar{1})$

segment BA $\quad BD \rightarrow B\alpha + \alpha D$ on $(\bar{1}11)$, etc.

The length of the resulting stair rods $\alpha\gamma$ [Fig. 18(b)] depends on the stacking fault energy and for Al will be $\sim 2b$ long, i.e., of the same order as the core size. The segments ABC, DEF are, thus, free to glide on $(11\bar{1})$ and $(\bar{1}11)$ as the edges AF, CD climb but, because they are dissociated, they cannot climb as easily as AF and CD. There are two possibilities for climb, as shown in Fig. 18(c), namely, either the dislocation will climb continuously, normal to its Burgers vector in the $(\bar{1}0\bar{1})$ plane or it will climb and slip so as to remain on the same (111) plane. Segments AF and CD will gradually be eliminated. Finally, the loop will appear, as shown in Fig. 18(d), as a diamond with all four sides dissociated. Particularly if the S.F.E. is high, climb as a diamond shape will continue, all four sides climbing at the same rate, until all available vacancies are exhausted. Such a loop can be recognized by the fact that the edges lie parallel to [011] and [110] with its major axis along [121] [Fig. 18(d)]. However, the loop may rotate on its glide cylinder so as to shorten the total length of dislocation line. In this case, the edges lie along $\langle 121 \rangle$, and the loop is now in the pure edge orientation. An example of this kind of loop is given in Fig. 9.

If the dislocations AF and CD climb in the (101) plane, the loop will no longer remain in one plane since part lies in (111) and part in (101). However, the segments ABC and DEF are free to glide on their respective {111} planes and could, therefore, slip so as to bring the whole loop into the (101) or some intermediate plane. This is favorable since the original segments ABC and DEF are thereby shortened. This mechanism is illustrated in Fig. 18(e). The above mechanism is a possible explanation of Takamura and Greenfield's observations[69] of diamond-shaped loops on {110}. Barnes *et al.*[57,60] have also observed diamond-shaped loops on {110} in Al after irradiation.

It is difficult experimentally to determine the exact plane of the loop unless special specimen tilting experiments can be done (see Appendix B). Use of a goniometer stage is essential to avoid ambiguous results. In alloys, the solute atoms may segregate to the dislocations and could play a role in determining the final orientation, e.g., solute atoms may actually cause rotation of the loop into the required habit plane for precipitation, as quenching defects are often observed to be preferential sites for precipitation.[19,38–41,44]

The diamond loops must always be perfect and are formed finally by *combined* climb and glide. The fact that diamond loops are commonly observed is indirect proof of preferential climb of the undissociated edge segments of a loop. The same is true for helical dislocations, as they also tend to climb into regular diamond shapes (Fig. 9).

7. DIRECT OBSERVATIONS OF CLIMB

Silcox and Whelan[70] were the first to present direct experimental evidence for climb by carrying out annealing experiments on quenched loops in pure Al. They observed that at 170°C and above, all the loops shrank. This was interpreted in terms of the loss of vacancies from loops and their diffusion to sinks (chiefly the foil surfaces). The process is, thus, that of climb whereby vacancies are emitted at jogs on the loop. In thin foils, Silcox and Whelan were able to ignore supersaturation effects (which would cause growth of loops) and, assuming the surfaces were infinite sinks, the rate of decrease of the loop radius r with time t is parabolic and of the form:

$$r = r_0[1 - t(\tau)]^{\frac{1}{2}} .$$

The "time constant" τ is given by $\tau = \tau_0 \exp(-E_D/kT)$ where E_D is the self-diffusion energy and $\tau_0 = r_0^2(Z\nu\, b^2\, \alpha)^{-1}$. Here, ν is the atomic frequency of vibration ($\sim 10^{13}$), b is the Burgers vector, α is a constant ($=64$ at 200°C for Al), and Z a coordination factor ($=11$). Figure 20 shows an experimental plot of the radius–time relationship for a shrinking loop,[23] from which the value of E_D was found to be 1.3 eV, agreeing with Silcox and Whelan's result and those obtained by other methods.[71,72] Attempts to determine E_D by investigations of the annealing of loops in bulk Al were not successful due to compli-

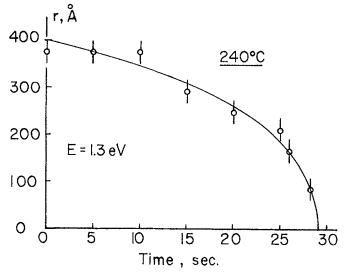

FIG. 20. The radius of a shrinking loop vs time during annealing in the electron microscope.

[69] J. Takamura and I. G. Greenfield, J. Appl. Phys. **3**, 247 (1962).

[70] J. Silcox and M. J. Whelan, Phil. Mag. **5**, 1 (1960).

[71] W. M. Lomer, *Vacancies and Other Point Defects in Metals* (Institute of Metals, London, 1958), p. 79.

[72] C. Panseri and T. Federighi, Phil. Mag. **3**, 1233 (1958).

cations arising from vacancy supersaturation effects; large loops were observed to grow at the expense of smaller ones.[70,73] These experiments confirmed that the second stage of annealing observed from E.R. measurements was due to the elimination of loops by climb.[71,74] The first and main drop in resistivity is due

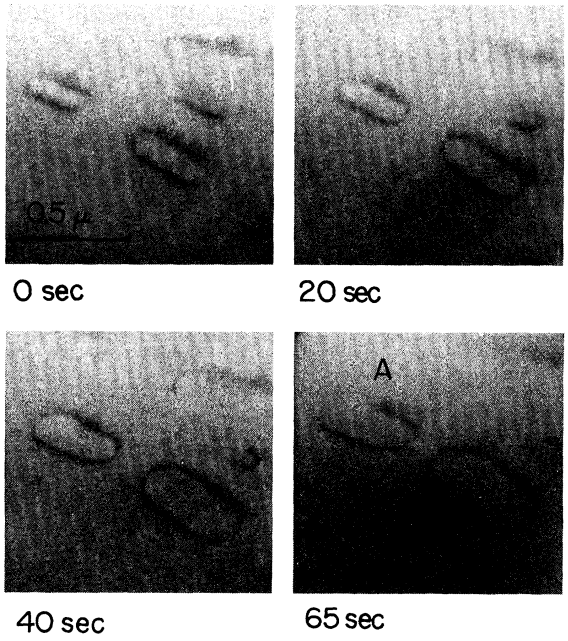

FIG. 21. Showing growth of loops in Al–5% Mg alloy during annealing at 365°C in the electron microscope.

to the migration and clustering of supersaturated vacancies. Similar results were obtained by Cotterill[25] on quenched gold except that the "second" annealing stage occurred in at least two parts. This may be associated with the impurity effects mentioned earlier. Cotterill was also able to determine experimentally the electrical resistivity of stacking faults and vacancies in Au by correlating observed resistivity values with the concentration and size of tetrahedra in the same material. He obtained $\rho_{SF} = [1.8 \pm 0.3] \times 10^{-13}\ \beta\ \Omega\ \text{cm}^2$ for a stacking fault density of $\beta\ \text{cm}^{-1}$ and a lower limit for the resistivity of vacancies at $\rho_r = [2.4 \pm 0.4] \times 10^{-6}\ \Omega$ cm at.% vacancies. This experimental value of ρ_{SF} agrees very well with Howie's calculated value[75] of $[2.5 \times 10^{-13}\ \beta\ \Omega\ \text{cm}^2]$, and the more recent result of de Jong and Koehler[68] $\{(1.3 \pm 0.4) \times 10^{-13}\ \beta\ \Omega\ \text{cm}^2\}$.

In contrast to pure Al, the behavior of loops in Al–5% Mg alloys is the same during annealing both bulk specimens and thin foils.[23] In both cases, loops (and helices) *grow*, e.g., Fig. 21. In other words, supersaturation conditions can be maintained in thin foils of this alloy. A similar result has been observed in Al–20% Ag.[41] The rate of growth $\dot{r} = dr/dt$ was observed to be constant even when a loop intersected the surface. Figure 22 shows a plot of $\dot{r}$ against $1/T$, from which the activation energy E_{-G} for the process is found to be 0.95 ± 0.05 eV[23] as compared to 1.3 eV for pure Al.[70] This result was interpreted in terms of the effect of the binding energy Mg-vacancy on the rate of climb.

In a two-component system the vacancy concentration x' is given by[71]

$$x' = A \exp\left[-E_f/kT\right](1 - 12c + 12c \exp\left[E_B/kT\right]),$$

where E_f is the vacancy formation energy in the pure metal and c is the atomic fraction of solute atoms. x' can be measured from the density and size of loops and x (for the pure metal) can be calculated from $x = A \exp\left[-E_f/kT\right]$, hence,

$$\exp\left(\frac{E_B}{kT}\right) = \left[\left(\frac{x'}{x} - 1\right) + 12c\right]\frac{1}{12c}.$$

The following shows an example of the value of E_B obtained from a bulk annealing experiment[23]:

Treatment	Loop density	Diam. (Å)	x	x'/x	E_B
Q + 60′ 183°C in bulk	1.4×10^{13}	2890	2.6×10^{-4}	3.1	0.10

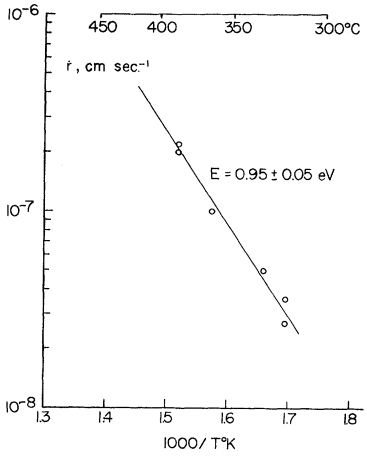

FIG. 22. Rate of increase in loop radius vs reciprocal of the absolute temperature for Al–5% Mg alloy. Results obtained from annealing experiments in the electron microscope.

The maximum value of E_B found by this method is 0.16 eV. However, measurements of x' are likely to be on the low side because only those vacancies which have gone to loops or helices have been counted.

[73] R. Vandervoort and J. Washburn, Phil. Mag. **5**, 24 (1960).
[74] T. Federighi and C. Panseri, Acta Met. **8**, 217 (1960).
[75] A. Howie, Phil. Mag. **5**, 251(1960).

From the kinetic data obtained from thin foil experiments we can write (Fig. 22):

$$E_{(-G)} = E_f + E_m + nE_B = 0.95 \pm 0.05 \text{ eV}.$$

If E_B is involved only in E_f or E_m, $n = 1$, but if E_B is equally active in E_f and E_m, $n = 2$. Putting $E_f = 0.76$ eV, $E_m = 0.54$ eV (values for pure Al), then the maximum value of $E_B = 0.4$ eV for Mg-vacancy "couple" diffusion. If the vacancies are trapped in a Mg-vacancy complex, the clusters must evaporate off vacancies, so we can write: $E_{-G} = E_f + E_m + 2E_B$. Putting in the values for E_{-G}, E_f, and E_m, E_b (min) is then 0.17 eV. This value agrees quite well with the bulk experimental results and also with the E.R. results given in Table II. The actual value of E_b depends upon the vacancy-solute atom configuration and is probably sensitive to quenching rate, temperature, and possibly composition.

Silcox[76] studied the annealing out of tetrahedra in quenched gold but, unlike loops in pure Al, continuous decrease in size of tetrahedra was not observed. The tetrahedra disappeared suddenly after heating to above 650°C.

Meshii and Kaufmann[77] determined the activation energy for elimination of tetrahedra to be 4.8 eV. Silcox[76] and Hirsch *et al.*[78] suggest that this high activation energy may result from annihilation by interstitial diffusion. Some evidence for this[78] was obtained by irradiating quenched gold with α particles at 20°C. This radiation produces mobile interstitials and they observed that tetrahedra disappeared with increasing dose. The tetrahedra are assumed to collapse after accretion of a critical number of interstitials has occurred by diffusion.

The interpretation of this experiment does not appear to be consistent with the observed simultaneous growth of vacancy tetrahedra and interstitial loops in irradiated copper.[56] Therefore, the mechanism of decomposition of perfect tetrahedra is still not clear.

8. EFFECT OF VACANCY CLUSTERING ON MECHANICAL PROPERTIES

Experimental information on quench hardening has been confused by inadequate control of variables such as: specimen diameter, purity, quenching conditions, aging temperature, and orientation of the specimen axis. Slight changes in these factors can cause important differences in the resulting quenched and aged substructure. The defect substructure in a quenched and aged crystal is, at best, complex, as was shown in Sec. 3. Typical colonies of loops in an aluminum specimen quenched from 600°C to −20°C then aged at 100°C are shown in Fig. 3.[35]

Even though quenching substructures are nonuniform and have certainly not been comparable in the experiments carried out at different laboratories, some general effects on mechanical properties are fairly well established:

(1) Little or no hardening except perhaps below 78°K is produced by excess vacancies as long as they remain dispersed or in clusters of no more than a few. Not only is there no change in yield stress for quenched copper[33,79] and gold[80] when tested without aging at 20°C or −196°C, but also there is not much change in the entire stress–strain curve.

(2) Very small clusters, perhaps involving ten to several hundred vacancies, such as those that are probably formed during electron irradiation of copper,[81] cause an increase in the yield stress but little change in the strain hardening rate. The entire stress–strain curve is just shifted to a slightly higher stress level.[33]

(3) Clusters large enough to become visible by transmission electron microscopy as "black spots," or collapsed clusters in the form of stacking fault tetrahedra, stacking fault loops, or perfect prismatic dislocations cause strong hardening.[79,80,82,83] For the smallest visible clusters, such as the "black spots" produced by neutron irradiation of copper or gold, the hardening is strongly temperature dependent.[84,85] The hardening produced by large loops or tetrahedra is rather insensitive to temperature of testing.[80,86] Loops or "black spots" also cause changes in the shape of the stress–strain curve and a less uniform distribution of plastic strain.[82,83,87] The hardening rate following the yield is increased for crystals oriented for single slip and reduced for the multiple slip [111] orientation.[33] These effects are illustrated by Figs. 23 and 24, which are shear stress vs shear

[76] J. Silcox, Ph.D. thesis, Cambridge University (1961).
[77] M. Meshii and J. W. Kauffman, Phil. Mag. **5**, 939 (1960).
[78] P. B. Hirsch, R. M. J. Cotterill, and M. W. Jones, *Proceedings of the 5th International Congress on Electron Microscopy* (Academic Press Inc., New York, 1962), p. F-3.
[79] H. Kimura, R. Maddin, and D. Kuhlmann-Wilsdorf, Acta Met. **7**, 154 (1959).
[80] M. Meshii and J. W. Kauffman, Acta Met. **7**, 180 (1959).
[81] M. J. Makin and T. H. Blewitt, Acta Met. **10**, 241 (1962).
[82] R. Maddin and A. H. Cottrell, Phil. Mag. **46**, 735 (1955).
[83] L. E. Tanner and R. Maddin, Acta. Met. **7**, 76 (1959).
[84] T. H. Blewitt, R. R. Coltman, D. K. Holmes, and T. S. Noggle, *Creep and Recovery of Metals* (American Society for Metals, Cleveland, 1957).
[85] M. J. Makin, AERE M/R 2080 Harwell, Berkshire, U. K. (1957).
[86] M. Wintenberger, Ann. Phys. **5**, 1185 (1960).
[87] A. K. Seeger, *Proceedings of the Second United Nations Conference on the Peaceful Use of Atomic Energy* (United Nations, Geneva, 1958), Vol. 6, p. 250.

strain curves for copper single-crystal wires which were quenched from 1060°C and aged for various times at 20°C before testing at 78°K.

Figure 25 shows the correlation between quench-age-hardening and the growth in size of clusters as observed by x-ray small angle scattering. The decay of excess resistivity, which represents primarily the disappearance of single vacancies and divacancies as they reach the clusters, is also shown.

9. THEORIES OF HARDENING

The actual defect substructures that exist in quenched and aged crystals are too complex to permit accurate quantitative predictions of the yield stress. However, order of magnitude calculations can be made by assuming that only one cluster or loop size is present and that these defects are uniformly dispersed throughout the crystal volume. These assumptions are probably more nearly true in some irradiated specimens where vacancy clusters are formed directly at displacement spikes.

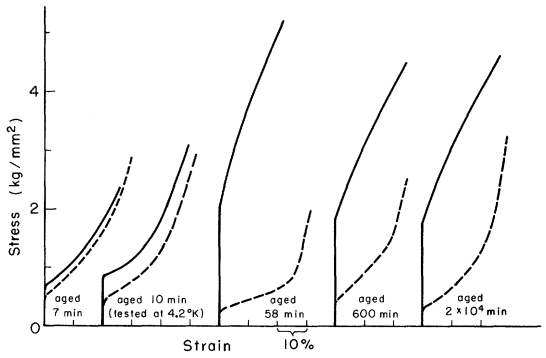

FIG. 23. Stress–strain curves for Cu showing effect of vacancy clusters for a single slip orientation of the tensile axis. Dashed curves are from a length of the same single crystal wire tested without quenching. Test temperature, 78°K.

Seeger[87] and later Friedel[88] have considered the motion of dislocations through a dispersion of voids or vacancy clusters of very small dimensions (such as those produced by heavy-particle irradiation at low temperature). For such small clusters, having dimensions not too much larger than atomic dimensions, the escape of the moving dislocation from the pinning points is thermally activated. The theories predict a hardening that increases with decreasing temperature. Friedel gives the temperature dependance as:

$$\tau = \tau_m(1 - T/T_c)^{\frac{3}{2}},$$

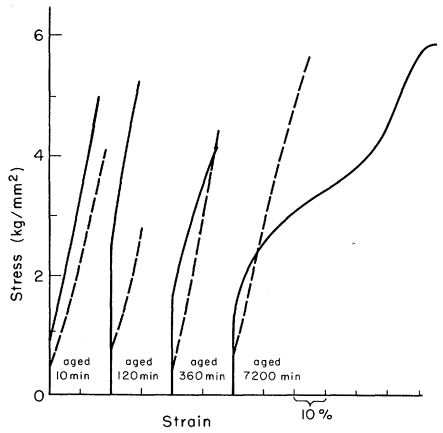

FIG. 24. Stress–strain curves for Cu showing effect of vacancy clusters for a multiple slip orientation (tensile axis [111]). Dashed curves are from a length of the same single crystal wire tested without the quench-age treatment. All tests at 78°K.

where τ_m is the hardening at absolute zero and T_c is a critical temperature which is well above room temperature if the energy for escape of the dislocation from a cluster is of the order of 1 eV. In this theory, $\tau_m l \simeq$ const where l is the average distance between clusters on the slip plane. Therefore, the magnitude of the hardening varies inversely with the distance between clusters on the slip plane.

Interactions between large dislocation loops and moving dislocations in the fcc structure have been considered in detail by Saada and Washburn.[89] If the loops are of the perfect prismatic type, a given moving dislocation will encounter loops of six different Burgers vectors. For loops of the stacking fault type, there will be four different Burgers vectors. It can be shown that two-thirds of the perfect loops, half of

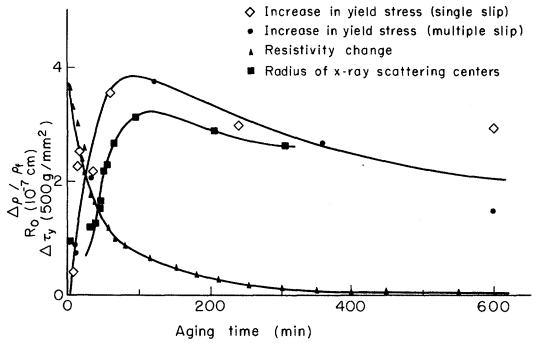

FIG. 25. Changes in yield stress, excess resistivity, and radius of small angle x-ray scattering centers in Cu during aging at 20°C after a rapid quench from 1070°C.

[88] J. Friedel, *Electron Microscopy and Strength of Crystals* (John Wiley & Sons, Inc., New York, 1963), p. 605.

[89] G. Saada and J. Washburn, *Proceedings at the 1962 Tokyo Symposium on Mechanical Aspects of Lattice Defects*, J. Phys. Soc. Japan (to be published).

the large imperfect loops, and all of the imperfect loops smaller than a critical size can form strong locking points on a moving dislocation. Dislocation reactions are possible that result in local reduction of the elastic strain energy of the dislocation or, in the case of small stacking fault loops, a step in the stacking fault must be formed.

Friedel[88] has analyzed in detail the way in which a moving dislocation behaves when passing through randomly situated loops that form attractive junctions with the dislocation. The line has a zig-zag form. (See Fig. 26.) The critical stress for continued motion is

$$\tau = (Gb/\beta)N^{\frac{2}{3}}R,$$

where N is the number of loops per unit volume, R is the average radius of the loops, and β is a constant

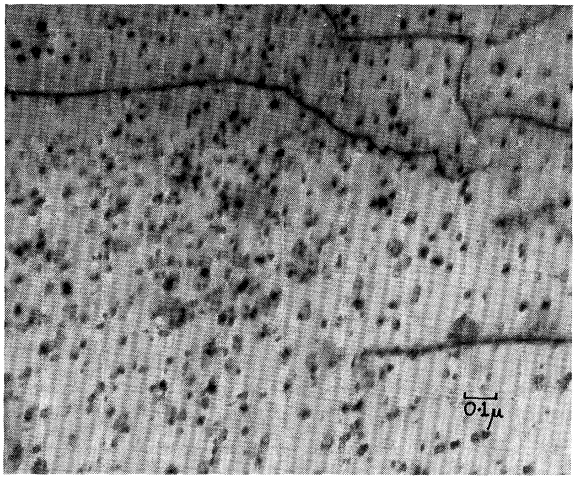

FIG. 26. Showing motion of a dislocation in Al containing dislocation loops. Notice cusps where the line is pinned by loops.

(about 4). The analysis predicts a temperature independent component of hardening in agreement with experiment.[80,86] For an aluminum crystal quenched from 600°C, N is of the order of 10^{15} and the average value of R is about 200 Å. Therefore, $\tau \approx 370$ g/mm^2, which is of the right magnitude to be consistent with the experiments of Maddin and Cottrell.[82]

10. THE STRESS–STRAIN CURVE

Plastic deformation gradually destroys the loop substructure.[76,90,91] When a moving dislocation meets a perfect loop with the same or opposite Burgers vector or a stacking fault loop on a {111} plane that does not contain the Burgers vector of the moving dislocation, then a part of the loop is destroyed. The moving dislocation acquires two large jogs that can usually glide away conservatively and a smaller loop is left behind. When a moving dislocation meets a stacking fault loop that lies on a plane parallel to the Burgers vector of the moving dislocation, then the stacking fault is swept away converting the loop to a perfect loop.[91] Therefore, glide on a single system can sweep away one-sixth of the perfect loops and one-half of the large stacking fault loops. The remaining large stacking fault loops are converted to perfect loops.

For very small loops or clusters, it is likely that these detailed considerations are not necessary. In this case, the vacancies may be able to disperse along a dislocation line by local or pipe diffusion producing long jogs that glide away conservatively.

Changes in strain hardening rate are probably related to this destruction of the quench-age substructure by moving dislocations. Figure 23 shows that for crystals oriented for easy glide the hardening rate immediately following the yield was greatly increased by quenching and aging for more than about one hour. However, the opposite effect was observed for the multiple-slip orientation (Fig. 24).

Both of these results can possibly be explained if it is assumed that the deformation in quench-aged crystals takes place at first by the growth of far fewer slip bands than in annealed crystals. This is known to be true for both irradiated[87,90,92,7] and quenched[83] materials. In crystals containing clusters or dislocation loops, plastic strain tends to take place by widening of already present glide bands rather than by frequent nucleation of new bands. This is almost certainly caused by the local softening effect resulting from the destruction of the loop substructure (Fig. 4).

In a single-crystal wire of small diameter oriented for single slip, the effect of a high yield stress and a less uniform distribution of the shear strain along its length may be to cause localized stress concentrations and bending movements that bring secondary systems into operation, almost immediately suppressing the easy glide. This may explain the greater initial hardening rate shown in Fig. 23 for the quench-aged easy glide oriented crystals. However, the effect seems to be associated only with fairly large clusters. At short aging times there was only a general increase in the stress level of the entire stress–strain curve,

[90] I. G. Greenfield and H. G. F. Wilsdorf, J. Appl. Phys. **32**, 827 (1961).

[91] I. G. Greenfield, *Proceedings of the 5th International Congress on Electron Microscopy* (Academic Press Inc., New York, 1962), p. F-4.

[92] B. L. Eyre, Phil. Mag. **7**, 1609 (1962).

as has been observed for irradiated copper.[90] Other factors, such as the diameter of the tensile specimen being employed, probably affect the results. A far more detailed model than any presently existing for yielding and hardening during easy glide is essential to a real understanding of these effects.

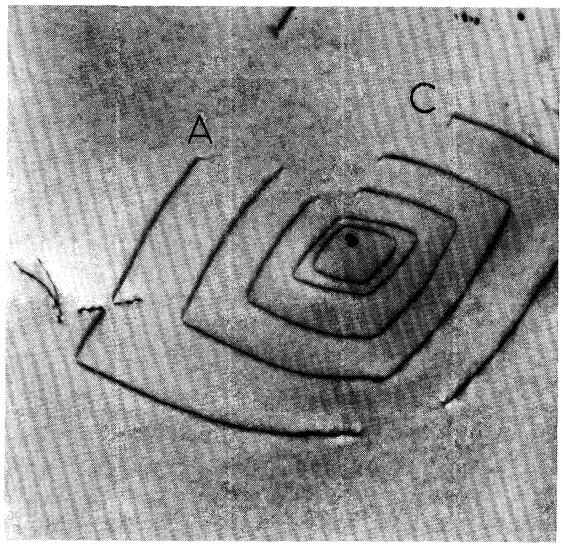

FIG. A1. Al–7% Mg alloy quenched from 500°C showing a climb source with concentric but not coplanar loops on (110). A loop has intersected the surface at A and C. After Embury and Nicholson[44] (courtesy Acta Met.).

In a crystal of [111] axis the growth of fewer slip bands might be expected to have just the opposite effect on hardening rate. Slip in any one part of the gauge length might, in this case, not involve all six of the slip systems. If slip bands on the six equally stressed systems are more or less isolated because of a small number of bands then there would be less cutting of one band by another. Fewer intersections should result in a less rapid accumulation of dislocation tangles and, therefore, a lower hardening rate, as is observed.

In this case, too, the explanation is certainly oversimplified. Further experiments correlating the distribution of plastic strain and the growth of slip bands with hardening rate and other parameters, such as specimen cross section, are clearly needed.

ACKNOWLEDGMENTS

We wish to thank our graduate students, F. Vinçotte, J. Strudel, A. Eikum, and J. Galligan for their contributions to this paper, and L. E. Thomas for providing Figs. 12 and 13. Financial assistance from the United States Atomic Energy Commission through the Inorganic Materials Research Division of the Lawrence Radiation Laboratory is gratefully acknowledged.

APPENDIX A

Dislocation Sources by Quenching

These have been observed in Al–Cu[16] and Al–Mg alloys,[30,93,44] systems in which E_b is not very small (Table II). A classical Frank–Read source was seen in Al–Cu[16] in which all screw segments had climbed into helices. Another new kind of source has been found recently, viz., the climb source.[30,93,44] It appears that precipitate particles are necessary for the nucleation of climb sources, e.g., as shown in Fig. A1. Simple sources show successive loops which lie on a pyramidal prism (Fig. A2) having {110} habit and contrast experiments show that their Burgers vectors are normal to those planes giving the characteristic diamond shapes discussed in Sec. 6. Screws may not act as climb sources because they are usually quickly converted into helices. The loops expand in the {110} planes by absorbing more vacancies since denudation of vacancy loops is apparent in regions around the source.

Westmacott *et al.*[93] observed more complicated configurations involving dislocations with more than one Burgers vector. These workers proposed that the origin of the climb source is a ⟨100⟩ dislocation from a precipitate which dissociates during climb as follows:

$$a\,[001] \rightarrow \tfrac{1}{2}\,a\,[011] + \tfrac{1}{2}\,a\,[0\bar{1}1] \text{ both in the (100)}$$
$$\rightarrow \tfrac{1}{2}\,a\,[101] + \tfrac{1}{2}\,a\,[\bar{1}01] \text{ both in the (010)}\,.$$

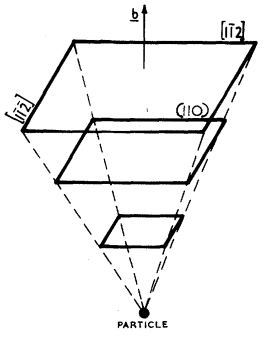

FIG. A2. Schematic illustration of the geometry of a pyramidal source such as that shown in Fig. A1. After Embury and Nicholson (Ref. 44) (courtesy Acta Met.).

For the reasons discussed in Sec. 6, loops other than those on {110} may be formed and it appears that whilst Westmacott *et al.* first proposed that their loops were on {100}, it is now felt[44] that these loops

[93] K. H. Westmacott, R. S. Barnes, and R. E. Smallman, Phil. Mag. 7, 1585 (1962).

may be concentrically arranged on irrational planes such that the directions of the bounding dislocations are given by the lines of intersection of the habit plane with the two {111} planes containing the Burgers vector of the loop.

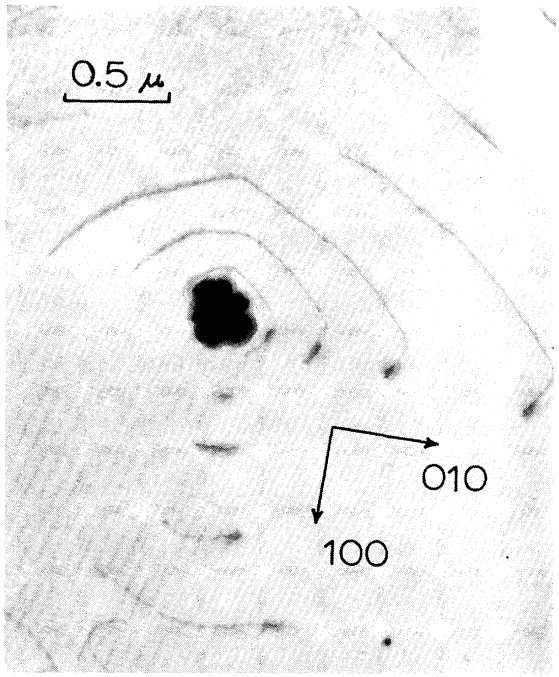

FIG. A3. Climb source in Al–5% Mg alloy quenched from 520°C and aged 94 h at 100°C.

These loops cannot be formed from the particles by a punching mechanism since they are always of the vacancy type and can be formed during isothermal aging. The sources are, thus, thought to be of the Bardeen–Herring kind.[94] Embury and Nicholson[44] showed that a high enough vacancy supersaturation must exist so that the resulting chemical stress is large enough to operate a source of length ≈ particle diameter. Such supersaturations are readily available by quenching and an excess of vacancies may already exist around particles if they are formed under tension, so repelling vacancies created by solute atoms going to the precipitate.

Many source configurations are possible depending on the kinds of interfacial dislocations present. The final result may also be complicated by interactions with other dislocations or by simultaneous operation of more than one source at a given precipitate. Figure A3 is an example of a configuration which may have formed either from a single-ended source or from loops which have been rotated relative to each other since the lines of intersection with the foil surfaces do not coincide.

[94] J. Bardeen and C. Herring, *Imperfections in Nearly Perfect Crystals* (John Wiley & Sons, Inc., New York, 1962), p. 261.

APPENDIX B

Determination of the Sense of Loops (i.e., vacancy or interstitial kind)

As a result of the development of the kinematical and dynamical theories of electron diffraction contrast,[3,4] it is now possible (under favorable circumstances) to determine the sense of the Burgers vector of dislocations. Thus, loops formed from vacancies or interstitials can be distinguished. Here, we shall follow the method recently presented by Mazey *et al.*[57] based on the dynamical theory of Howie and Whelan.[4]

In fcc metals the vacancy loop and interstitial loop can be formed from Frank sessile loops by reactions such as:

$$\tfrac{1}{3}[111] + \tfrac{1}{6}[\bar{2}11] = \tfrac{1}{2}[011] \text{ vacancy}$$

$$\tfrac{1}{3}[\bar{1}\bar{1}\bar{1}] + \tfrac{1}{6}[11\bar{2}] + \tfrac{1}{6}[1\bar{2}1] = \tfrac{1}{2}[0\bar{1}\bar{1}] \text{ interstitial}$$

i.e., the Burgers vectors are the same but are opposite in sense (Fig. B1).

Figure B1 shows the diagram used by Mazey *et al.* to define the Burgers vectors. The direction of the edge component of the Burgers vector of a loop with respect to the sense around the loop (taken as positive) is given by the right-hand and left-hand rules[95] for vacancy and interstitial loops, respectively.

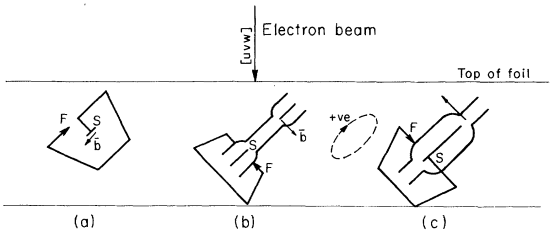

FIG. B1. Sketch defining the convention of the Burgers vectors of (a) an edge dislocation line, (b) a vacancy loop, and (c) an interstitial loop. After Mazey *et al.*[57]

"Taking the positive direction around a loop to be clockwise, vacancy loops have a Burgers vector with a positive component normal to the slip plane in the downwards sense (making an acute angle to the direction of viewing) whilst interstitial loops have a Burgers vector with a positive component along the upwards normal to the slip plane." (Fig. B1.)

[95] B. A. Bilby, R. Bullough, and E. Smith, Proc. Roy. Soc. (London) **A231**, 263 (1955).

Now the condition for visibility of a dislocation is that $\mathbf{g}\cdot\mathbf{b} \neq 0$. ($\mathbf{g}$ is the reciprocal lattice vector corresponding to the reflecting plane producing contrast.) Since the image of a dislocation is displaced to one side of the true position of the dislocation,[3,4] determination of the image position for a given

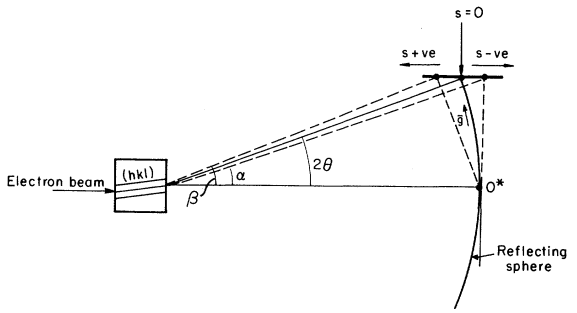

FIG. B2. Sketch showing the deviation s from the reflecting position corresponding to the angular deviations $(2\theta - \alpha)$, $(\beta - 2\theta)$ from the Bragg condition. s is positive when the reciprocal lattice point corresponding to $\mathbf{g}$ lies inside the reflecting sphere (angle of incidence greater than the Bragg angle).

reflection, $\mathbf{g}$, and sign of the deviation parameter s enables the sign of $\mathbf{g}\cdot\mathbf{b}$ and, hence, the sense of $\mathbf{b}$ to be determined. Figure B2 shows the reflecting conditions corresponding to positive and negative values of s, and Fig. B3 shows the sense of the displacement of the image when s is positive or negative using the sign convention given above. For a loop, the image will either be completely inside or outside the loop and when $(\mathbf{g}\cdot\mathbf{b})s$ is positive, the loop will appear larger than when $(\mathbf{g}\cdot\mathbf{b})s$ is negative. Thus, observations of the change in size of a loop on either side of an extinction contour ($\mathbf{g}$ fixed, s changing sign) or an absorption band (s constant, $\mathbf{g}$ changing sign) by tilting the specimen enables the sense of $\mathbf{b}$ to be obtained.

In order to determine the values of $\mathbf{g}\cdot\mathbf{b}$ and the sign of s, the diffraction pattern must be properly indexed so that $\mathbf{g}$ is given the right sign and, hence, the indices of the normal upward from the foil surface are known uniquely. Groves and Whelan[96] point out that the object and diffraction pattern differ from the image and the diffraction pattern by one inversion. Thus, besides correcting for rotation (due to the reduction in lens current when changing from image to diffraction pattern), the diffraction pattern must also be further rotated by 180°.

In practice, loops must be large enough so that their habit plane (and, therefore, Burgers vectors) may be identified. Unique identification is facilitated if a nonsymmetrical orientation is viewed. [E.g., if the foil is in $[0\bar{1}1]$, loops on inclined $(\bar{1}\bar{1}1)$ and $(1\bar{1}1)$ would appear to be in the same inclination in the image (hence, there are six possible $\langle 110\rangle$ Burgers vectors) leading to ambiguity in interpretation.] The sense of inclination of the habit plane with respect to the foil surface must be known if the diffraction pattern is to be unambiguously indexed. This can be determined by observing the change in projected area of loops during tilting in a known direction (Mazey *et al.*[57] used a 15° wedge to do this), and plotting the results stereographically. An accurate goniometer specimen stage would greatly facilitate determination of the orientation uniquely. Once all parameters are established, the diffraction pattern can be unambiguously indexed and the respective $\mathbf{g}$ operators and, hence, $\mathbf{b}$ can be determined. If $[\bar{u}\bar{v}\bar{w}]$ is the normal upward to the foil (obtained from the diffraction pattern in the usual way) and the $\mathbf{b}$'s are in the same sense as $[\bar{u}\bar{v}\bar{w}]$, (Fig. B1) the images correspond to interstitial loops. If the $\mathbf{b}$'s are in the opposite sense, the loops must be of the vacancy kind.

Experimentally, the procedure is tedious and difficult but it is a method which can be used for loops or dislocations of any kind and it enabled Mazey *et al.*[57] to show that in Al bombarded with 38-MeV α particles (He^{2+} ions) the loops were predominantly of the interstitial kind. Single-crystal experiments choosing suitable orientations would facilitate identification. Simpler methods may be used for special cases,[97] and for noncubic crystals, e.g., in graphite[98,99] where the Burgers vectors of interstitial and vacancy loops are not merely of opposite sense.

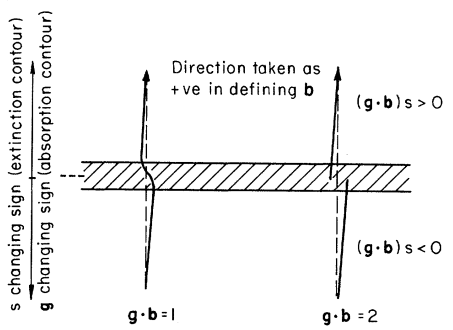

FIG. B3. Showing the sense of displacement of the image when $(\mathbf{g}\cdot\mathbf{b})s$ changes sign across either an extinction contour or an absorption band for the convention shown in B1. After Howie and Whelan (Ref. 4).

[96] G. W. Groves and M. J. Whelan, Phil. Mag. **7**, 1603 (1962).

[97] G. W. Groves and A. Kelly, Phil. Mag. **6**, 1527 (1961).

[98] G. K. Williamson and C. Baker, Phil. Mag. **6**, 313 (1961).

[99] S. Amelinckx and P. Delavignette, Phys. Rev. Letters **5**, 50 (1960).

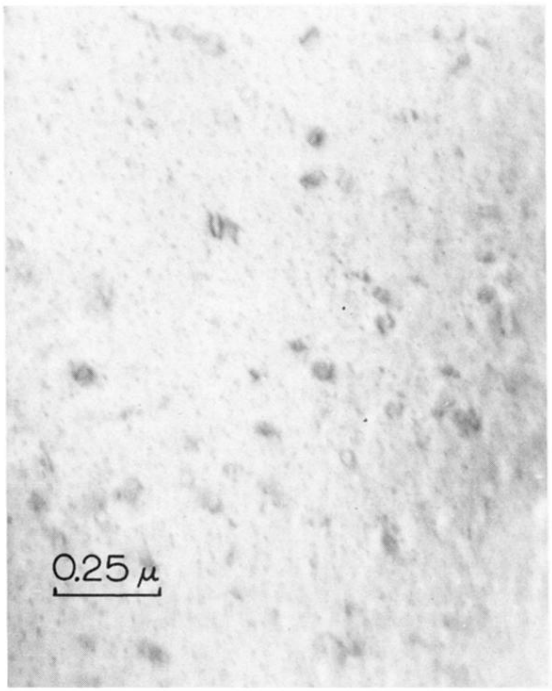

FIG. 1. Dislocation loops and "black dot" defect in O.F.H.C. copper quenched from 1000 °C and aged 1 h at 100 °C.

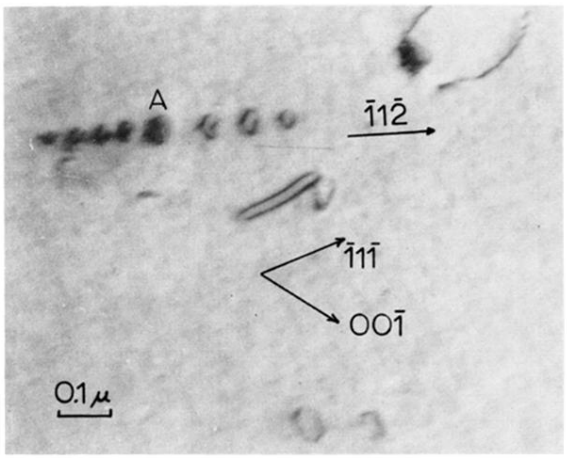

FIG. 10. Cu–0.5 at. % Ag quenched from 1065°C and aged 1 h at 100°C, showing a row of loops punched from the region A. The loops diminish in size with distance from the origin indicating that they are of the interstitial type.

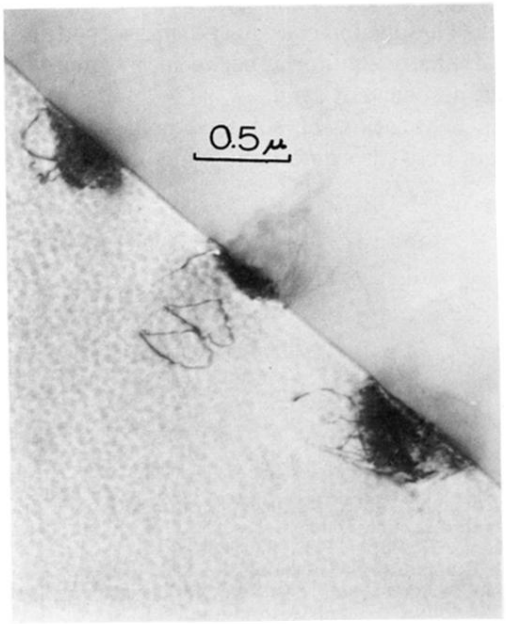

FIG. 11. Al–5 wt. % Mg quenched from 520°C and aged 70 h at 100°C, showing dislocation sources and punched loops originating from precipitates in the grain boundary.

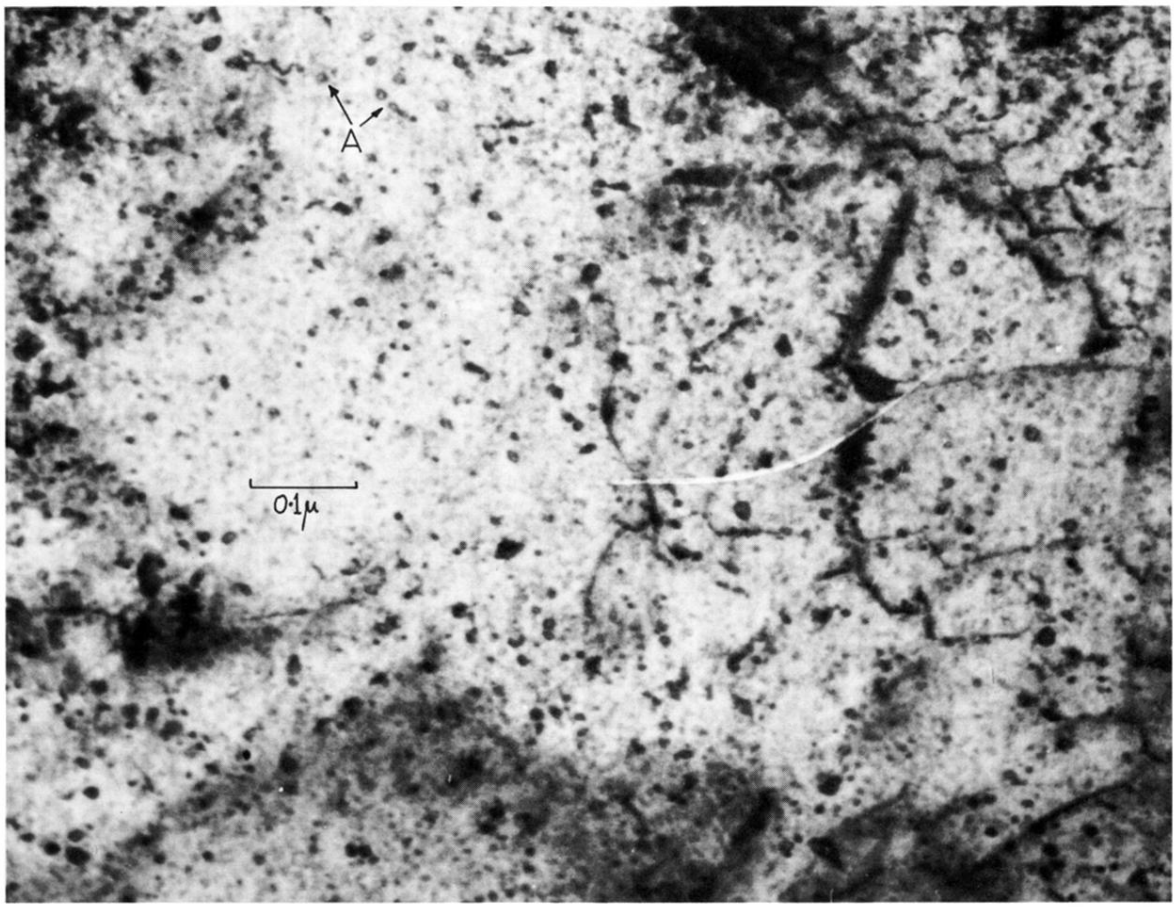

FIG. 12. High purity Nb annealed 1780°F and bombardment with 2×10^{17} Cs ions cm^{-2} (3.0 keV) at liquid nitrogen. Loops can be resolved at A (courtesy L. E. Thomas, Rocketdyne).

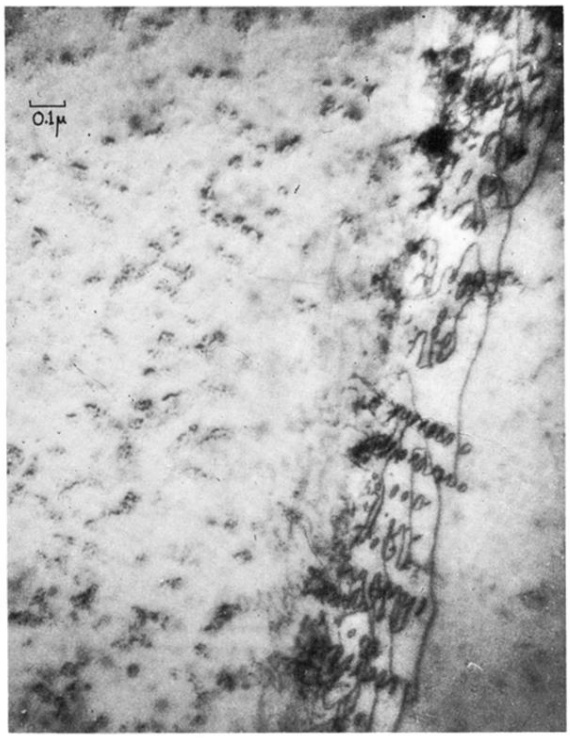

FIG. 13. As Fig. 12, showing helices and rows of loops emitted from a boundary. Notice clusters of black spot defects (courtesy L. E. Thomas, Rocketdyne).

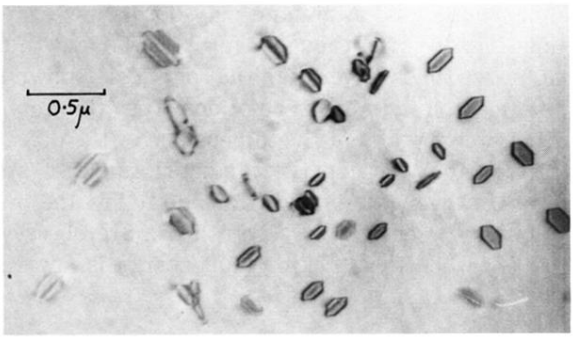

(a)

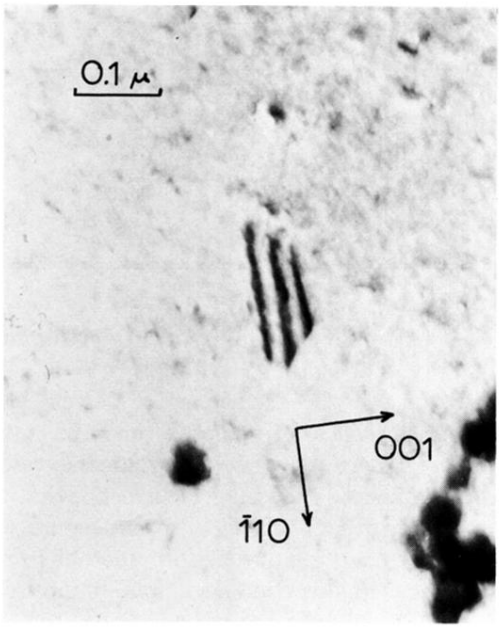

(b)

FIG. 16. (a) Frank loops in Al purity 99.999% quenched from 600°C to −20°C aged 5 sec 100°C. (b) A large truncated hexagonal Frank loop in Cu–2 at. % Ag quenched from 1000°C and aged 1 h at 100°C.

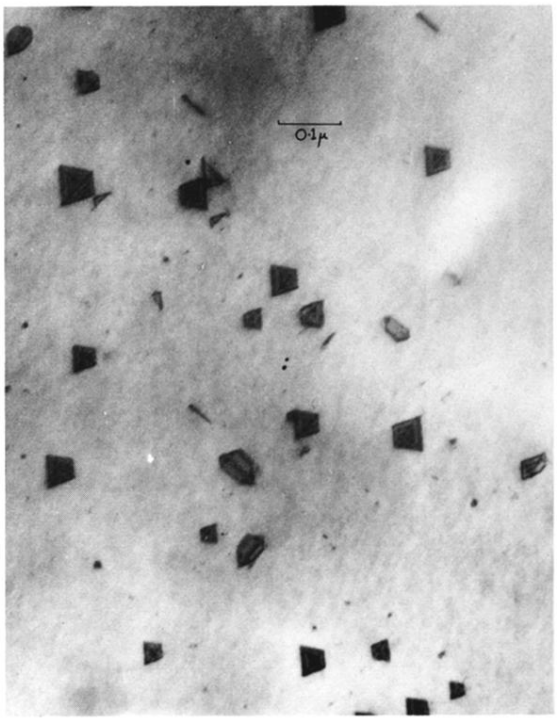

FIG. 17. Tetrahedra in quenched gold; after Silcox and Hirsch[24] (courtesy Phil. Mag.).

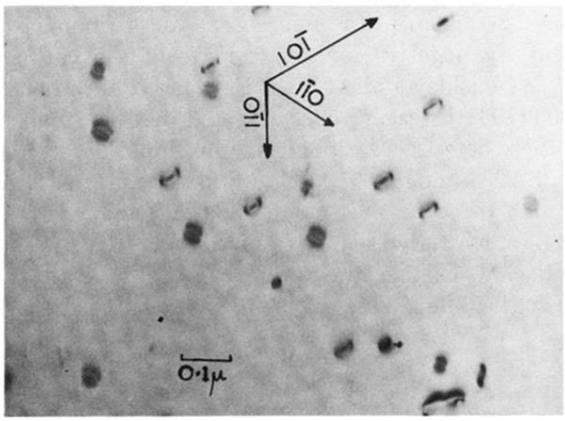

FIG. 2. [111] Al single crystal quenched from 600°C. Operating reflection $0\bar{1}1$. Notice that no loops are visible on (111) and ($\bar{1}11$) indicating that the loops are all of the stacking fault type with $a/3$ ⟨111⟩ Burgers vectors.

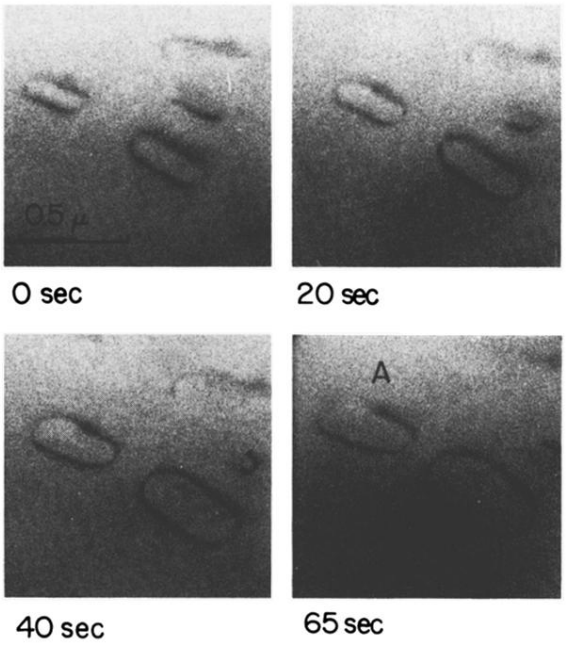

FIG. 21. Showing growth of loops in Al–5% Mg alloy during annealing at 365°C in the electron microscope.

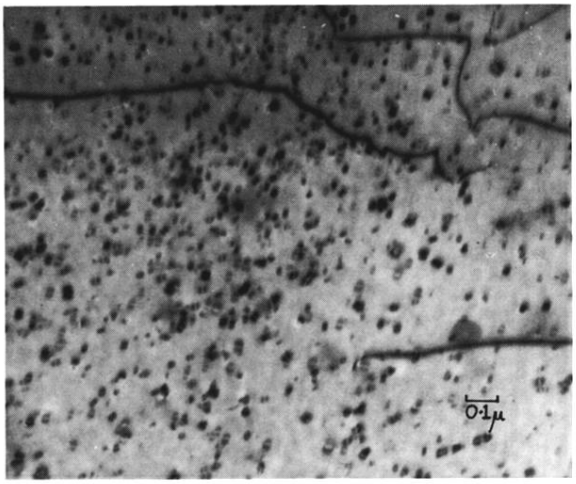

FIG. 26. Showing motion of a dislocation in Al containing dislocation loops. Notice cusps where the line is pinned by loops.

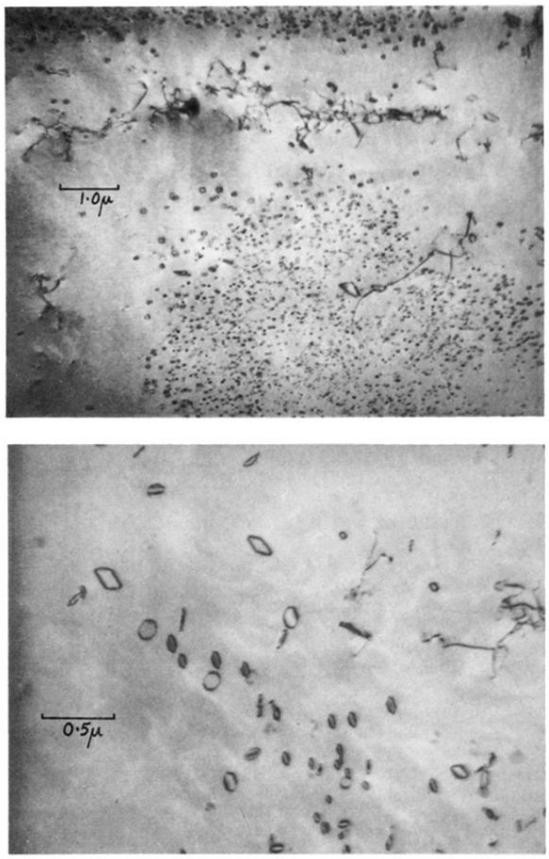

FIG. 3. (a) Showing colonies of loops in Al quenched from 600°C to −20°C, aged 5 sec 100°C (purity 99.999%). Notice larger loops at periphery of the colonies. (b) Enlarged view of edge of colony showing Frank loops as well as perfect diamond shaped loops.

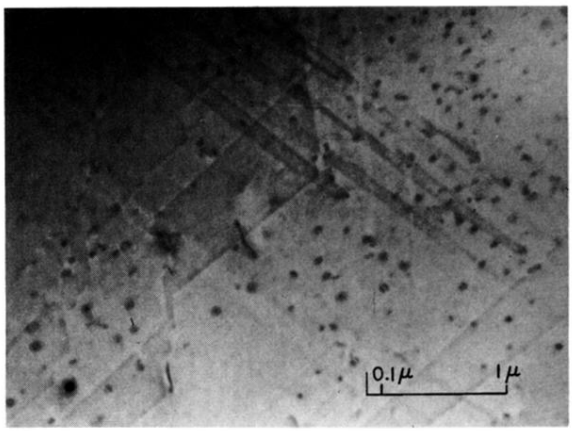

FIG. 4. Motion of dislocations with large jogs acquired by annihilation of loops (Courtesy ASM "Strengthening Mechanisms in Solids" 1962, p. 64).

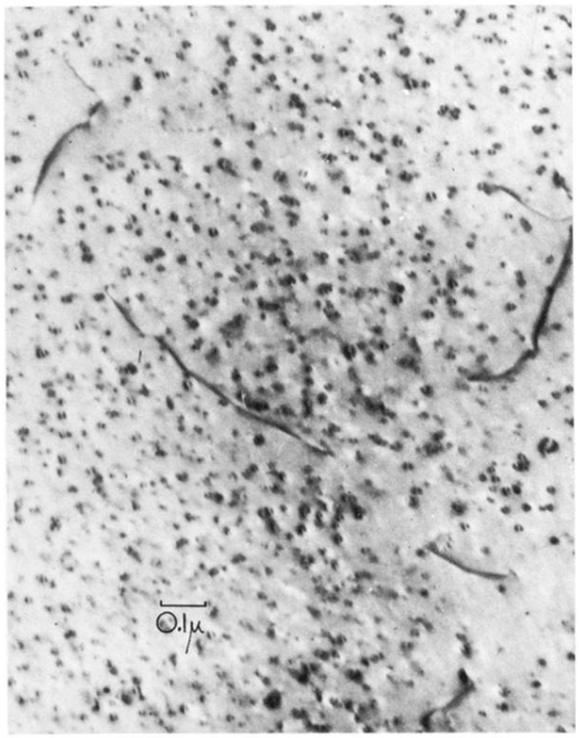

FIG. 5. Al–10% Zn alloy quenched from 580°C[14] (courtesy Phil. Mag).

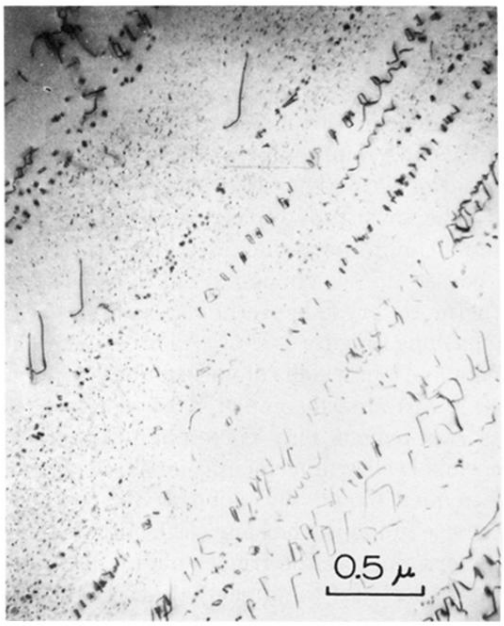

(a)

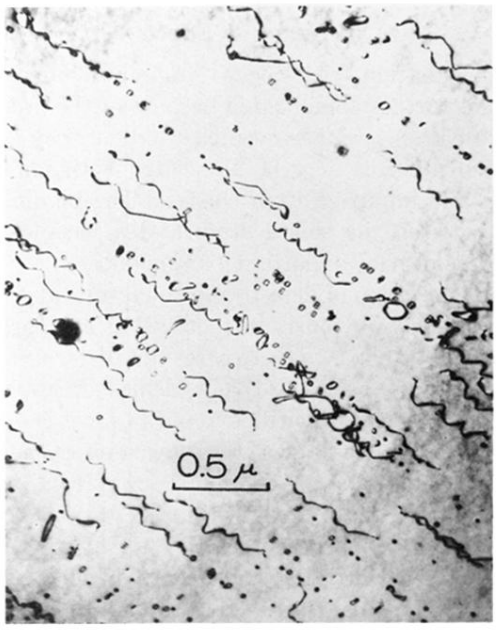

(b)

FIG. 6. (a) Al–5% Mg alloy quenched from 550°C deformed 3% aged 11 min at 20°C and further deformed 11%. Notice columns of large loops aligned along ⟨110⟩. (b) Al–5% Mg alloy quenched from 550°C. Comparison with Fig. 6(a) shows that the helices present here break down into loops as a result of deformation.

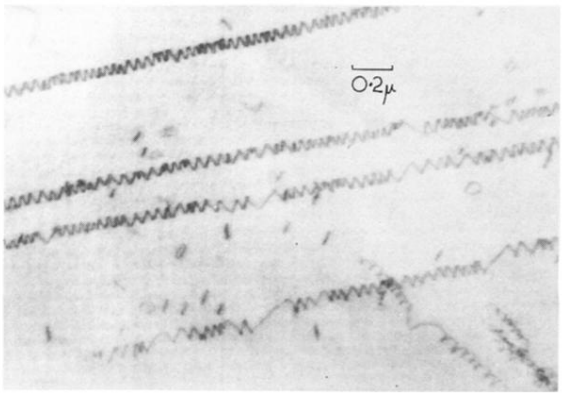

FIG. 8. Long regular helices in Al–4% Cu after quenching from 540°C[15] (courtesy Phil. Mag.).

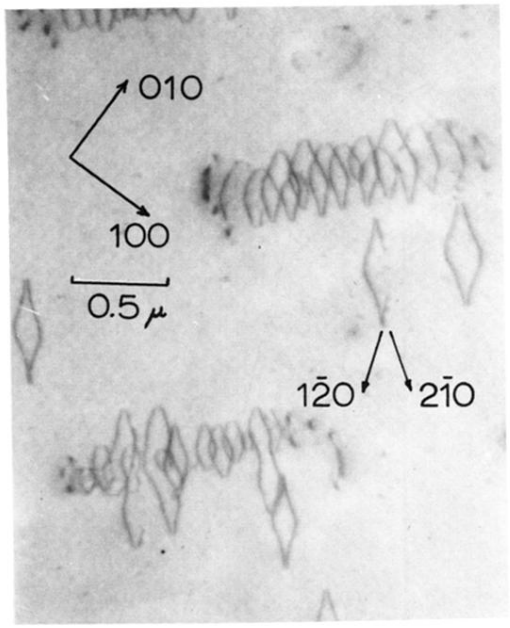

FIG. 9. Diamond-shaped loops and helices in Al–5% Mg quenched from 520°C and aged 94 h at 100°C. The most probable plane of the loops is (111) or ($\bar{1}\bar{1}$1).

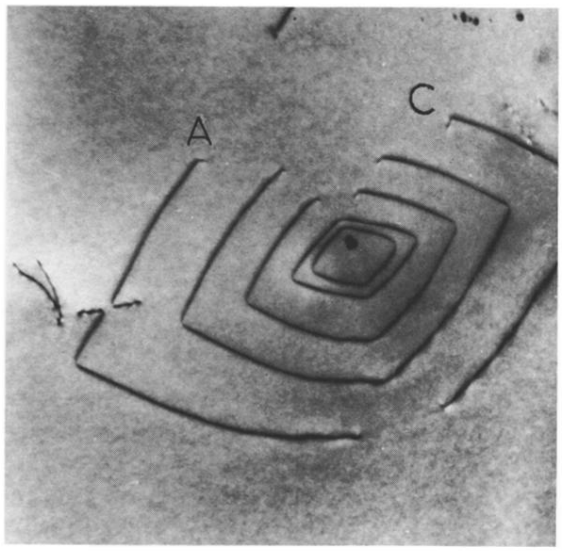

FIG. A1. Al–7% Mg alloy quenched from 500°C showing a climb source with concentric but not coplanar loops on (110). A loop has intersected the surface at A and C. After Embury and Nicholson[44] (courtesy Acta Met.).

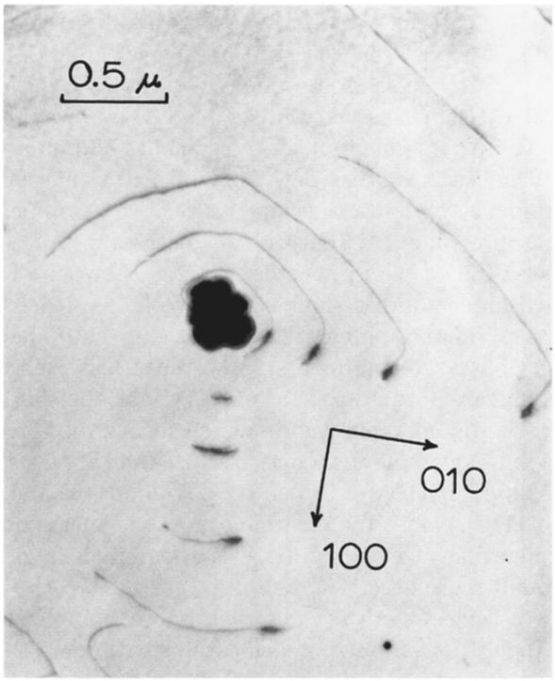

FIG. A3. Climb source in Al–5% Mg alloy quenched from 520°C and aged 94 h at 100°C.